

People's Democratic Republic of Algeria
Ministry of Higher Education and Scientific Research
University M'Hamed BOUGARA – Boumerdes



Institute of Electrical and Electronic Engineering
Department of Power and Control

Final Year Project Report Presented in Partial Fulfilment of
the Requirements of the Degree of

‘MASTER’

In Electrical and Electronic Engineering

Option: Telecommunications

Title:

**A Compact Quad Bands Patch Antenna And
MIMO Antenna System For Wireless
Communications**

Presented By:

- **Lokmane DIBES**
- **Cherif ADDAR**

Supervisor: **Dr F. Mouhouche**

Registration Number:...../2023

Dedication

I would like to dedicate this work to
Everyone who is near and dear to my heart

Cherif Addar

Dedication

I would like to dedicate this work to Everyone who is near and dear to my heart, starting with My Family Until to my teacher who helped me a lot Thank You So Much

Lokmane Dibes

Table of content

Abstract	1
General Introduction	2
Chapter 1: Generalities of Microstrip Antennas	4
1.1 Introduction.....	4
1.2 Microstrip antenna.....	4
1.2.1 History.....	4
1.2.2 Basic structure.....	4
1.2.3 Principle of Operation.....	5
1.2.4 Microstrip Antenna Feeding Method.....	6
1.2.4.1 Contacting feed.....	6
1.2.4.2 Non-Contacting Feed.....	7
1.2.5 Method Analysis.....	7
1.2.6 Antenna Parameters.....	8
1.2.6.1 Input Impedance.....	8
1.2.6.2 Directivity.....	9
1.2.6.3 Efficiency.....	9
1.2.6.4 Gain.....	9
1.2.6.5 Radiation Pattern.....	10
1.2.7 Advantages and disadvantages of Microstrip antenna.....	11
1.3 Introduction to multiple input multiple output systems (MIMO).....	11
1.3.1 introduction	11
1.3.2 Techniques of isolation.....	11
1.3.2.a Frequency diversity.....	11
1.3.2.b Time diversity	12

1.3.2.c Space diversity.....	12
1.3.3 Mutual Coupling.....	12
1.3.4 MIMO Application.....	13
1.3.4.a Data Rate Extension.....	12
1.3.4.b Power Saving.....	13
1.3.4.c Capacity Enhancement.....	13
 Chapter 2: A compact quad bands spiral monopole antenna	14
2.1 Introduction	14
2.2 Antenna Design	14
2.2.1 Parametric study	16
• Effect of Q	17
• Effect of outer ring Q1.....	18
• Effect of Q3.....	19
• Effect of Q4.....	19
2.2.2 Current Distribution.....	20
2.3 Fabrication and measurements	21
 Chapter 3: Compact quad band MIMO antenna for WiMAX and C applications.....	24
3.1 Introductions.....	24
3.2 DESIGN OF MIMO ANTENNA	24
3.3 Results and discussions.....	27
3.3.1 The input reflection coefficient	27

3.3.2 Parametric study.....	28
Effect of M_0	28
Effect of M	29
3.3.3 The current distribution.....	30
3.3.4 The radiation pattern.....	31
General Conclusion	36

List of figures

Figure 1.1: Basic microstrip patch antenna structure

Figure 1.2: Basic microstrip antenna configurations

Figure 1.3: Fringing fields in patch antennas

Figure 1.4: Four common feeding methods of microstrip patch antenna.

Figure 1.5: Method Analysis

Figure 1.6: Radiation pattern in spherical coordinates.

Figure 2.1.1: Evolution steps Ant-A

Figure 2.1.1.1: Simulated input reflection coefficient Ant-A.

Figure 2.1.2: Evolution steps Ant-B

Figure 2.1.2.1: Simulated input reflection coefficient Ant-B.

Figure 2.1.3: Evolution steps Ant-C

Figure 2.1.3.1: Simulated input reflection coefficient Ant-C

Figure 2.1.4: Evolution steps Ant-D

Figure 2.3.4.1: Simulated input reflection coefficient Ant-D

Figure 2.1.5: Evolution steps Ant-E

Figure 2.1.5.1: Simulated input reflection coefficient Ant-E.

Figure 2.1.6: Evolution steps Ant-F

Figure 2.1.6.1: Simulated input reflection coefficient Ant-F

Figure 2.1: Geometry of the proposed antenna. Top and Bottom view.

Figure 2.2: Evolution steps of the proposed antenna

Figure 2.3: Simulated input reflection coefficient of different stages of the proposed antenna.

Figure 2.4: Simulated the input reflection coefficient of the final structure.

Figure 2.5: Simulated input reflection coefficient for various Q

Figure 2.6: Simulated input reflection coefficient for different values Q1

Figure 2.7: Effect of Q3 on the (S11)

Figure 2.8: Effect of Q4 on the (S11)

Figure 2.9: Surface current distribution of the proposed antenna at (a) 1.36 GHz, (b) 2.5 GHz, (c) 3.63 GHz and (c) 4.15 GHz.

Figure 2.10: Simulated radiation patterns of the proposed quad-band antenna.

Figure 2.11: The simulated gain at four band frequencies of the proposed design

Figure 2.12: Fabricated prototype of designed antenna (A) front view (B) back view

Figure 2.13: Measured and simulated input reflection coefficient

Figure 3.1: Geometry of the proposed antenna (A) front view(B) back view.

Figure 3.2: Evolution structures of the proposed Quad band-MIMO antenna

Figure 3.3: Simulated (a) S11 (dB) (b) S21 (dB) response for different stages of the proposed MIMO antenna.

Figure 3.4: Simulated S11/S21 of the final structure.

Figure 3.5: Simulated S11/S21 for different values of M0

Figure 3.6: Simulated S11/S21 for various M

Figure 3.7: The surface current density of the proposed quad band MIMO antenna.

Figure 3.8: Simulated radiation patterns of the proposed MIMO antenna at 1.39, 2.5, 3.5and 4.02 GHz for port-1.

Figure 3.9: Realized gain characteristics of the proposed MIMO antenna.

Figure 3.10: Simulated ECC for the proposed MIMO antenna

Figure 3.11: Diversity gain of the proposed MIMO antenna.

List of Tables

Table 1.1: Comparison between different patch antenna feeding techniques

Table 2.1: Detailed parameters antenna.

Table 2.2: Comparison of our antenna with the existing antennas.

Table 3.1: Geometric dimensions of the proposed antenna

Table 3.2: Comparison of different antennas with the designed antenna

Abstract

This work presents a compact quad band MIMO antenna for wireless communication systems that is developed and investigated. The proposed MIMO antenna structure is composed of two adjacent identical antenna elements which are fed through microstrip lines. The single element of the MIMO system is the spiral monopole antenna. The quad bands are attained by introducing circular ring slots in a circular patch antenna to get a new form of spiral antenna. The proposed single antenna has a dimensions of $14 \times 18 \text{ mm}^2$. The results show that the single antenna element operates at (1.39), (2.5), (3.63) and 4.15GHz for WiMAX and C band. It is also observed from the results that the antenna offers good radiation characteristics for the frequency band of interest.

Furthermore, a 2×2 MIMO antenna is designed by utilizing the polarization diversity technique. The two spiral elements are placed orthogonally and an inverted L-shaped are placed between them to improve the isolation performance. Moreover, the proposed MIMO antenna operates (1.39), (2.5), (3.52) and 4.02 GHZ for WiMAX and C band applications. The isolation of the proposed antenna is higher than 15 dB, and the antenna maintains relatively stable radiation characteristics and gain, as well as a lower envelope correlation coefficient (ECC less than 0.2).

General Introduction

Antennas are devices designed to transmit and receive electromagnetic waves. They play a crucial role in various communication systems, enabling the wireless transmission of information over long distances. Antennas are widely used in applications such as radio and television broadcasting, wireless communication networks, radar systems, satellite communications, and more.

One type of antenna that has gained significant popularity is the microstrip antenna. Microstrip antennas are compact and lightweight, making them suitable for integration into small electronic devices. They consist of a metallic patch or strip placed on a dielectric substrate, which is usually a printed circuit board (PCB). The patch and the substrate create a resonant structure that radiates and receives electromagnetic waves.

Microstrip antennas offer several advantages, including ease of fabrication, low cost, and compatibility with modern PCB manufacturing techniques. They find applications in mobile phones, Wi-Fi routers, satellite communication systems, automotive systems, and many other wireless devices. Despite their small size, microstrip antennas can achieve reasonable performance in terms of Multi-bands, radiation efficiency, gain, and bandwidth.

Another important advancement in antenna technology is Multiple-Input Multiple-Output (MIMO) antennas. MIMO technology utilizes multiple antennas at both the transmitter and receiver ends to enhance wireless communication performance. It takes advantage of spatial diversity and multipath propagation to improve data throughput, increase reliability, and mitigate interference.

MIMO antennas employ antenna arrays with multiple elements, which can be arranged in various configurations, such as linear, planar, or conformal arrays. These arrays enable simultaneous transmission and reception of multiple data streams, effectively increasing the capacity and spectral efficiency of wireless communication systems. MIMO technology is widely used in modern wireless standards like 4G LTE, 5G, and Wi-Fi, enabling higher data rates and improved user experiences.

This report contains three chapters as follows:

Chapter1: review of basic concepts of microstrip antenna theories and MIMO system

Chapter2: provides the steps of designing quad band spiral monopole patch antenna operating at 1.63Ghz, 2.5Ghz, 3,63Ghz, and 4.15Ghz

In addition, an extensive parametric study for the proposed structure is carried out in order to have a better understanding of operating mechanism.

Chapter 3: we will present the design and simulation the MIMO system by using the two identical quad band spiral antennas.

The performances of quad band MIMO antenna will be discussed in details

Finally, a conclusion and some suggestions for future scope are presented

Chapter 1

Generalities of Microstrip Antennas.

1.1 Introduction

Microstrip patch antennas (MPA) are a class of planar antennas which have been investigated and advanced widely in the last four eras. They have become favorites among antenna designers and have been used in many applications in wireless communication systems, both in the military and in the commercial sector. The Microstrip antenna will absolutely continue to find many uses in the future due to its numerous distinctive and attractive qualities (e.g., lightweight, cheap cost, ease of fabrication, and compatibility with integrated circuits) [1].

In this chapter, some useful concepts on Microstrip antenna, its behavior and the theory behind main techniques of miniaturization are described in details.

1.2 Microstrip antenna

1.2.1 History

The origin of the microstrip antennas apparently dates back to 1953, when Deschamps proposed to feed an array of printed antenna elements using microstrip feed lines. The printed elements introduced there were not microstrip patches, but flared planar horns. A patent right was won by Vaissinot and Gutton in 1955. However the first implementation came into existence in 1970's when Robert E. Munson and some of his fellow researchers developed it using a low loss substrate[1].

1.2.2 Basic structure

In its most basic form, a Microstrip patch antenna consists of a radiating patch on one side of a dielectric substrate which has a ground plane on the other side as shown in Figure 1.1

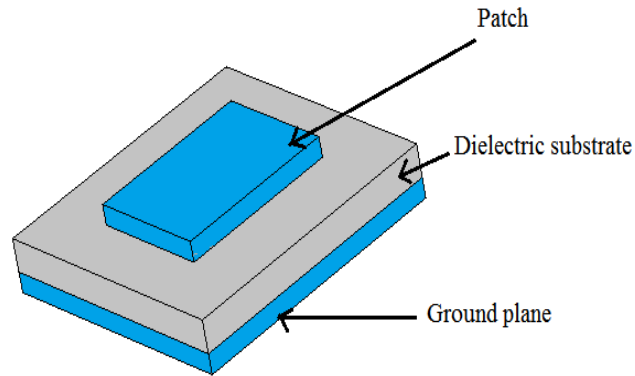


Figure 1.1 Basic microstrip patch antenna structure [2].

There are a large number of shapes of Microstrip patch antennas; they have been designed to match specific characteristics. Some of the common types are shown in **Figure 1.2**, the most common types are rectangular, square, and circular patches.

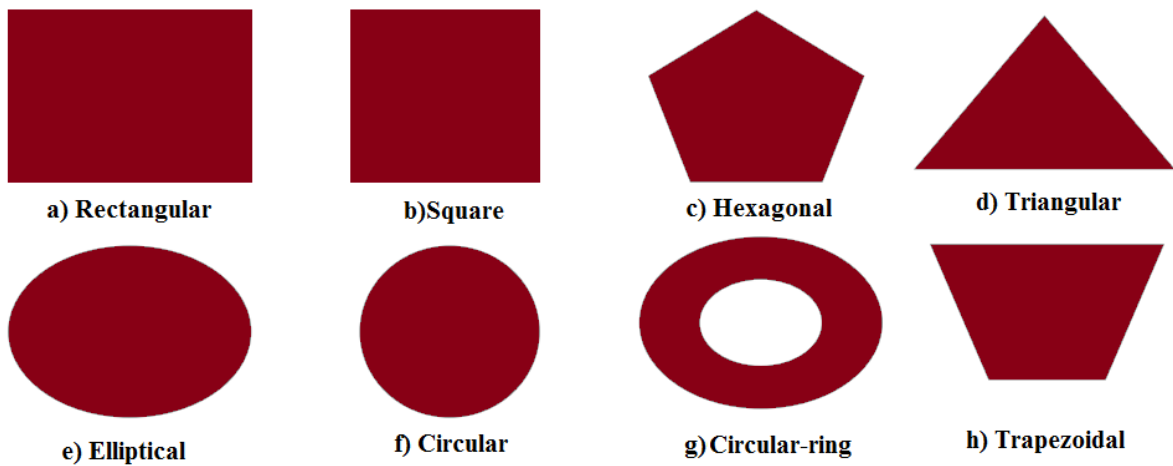


Figure 1.2 Basic microstrip antenna configurations [3].

1.2.3 Principle of Operation

The fringing fields around the microstrip antenna are responsible for the radiation. This is due to the fringing E-fields on the edge of the patch antenna which are in phase. This causes them to add up and produce electromagnetic wave radiation. The current also adds up in phase; however, in the ground plane an equal current but with opposite direction, which cancels the radiation therefore, the microstrip patch antenna is considered as a "voltage radiator" [4].

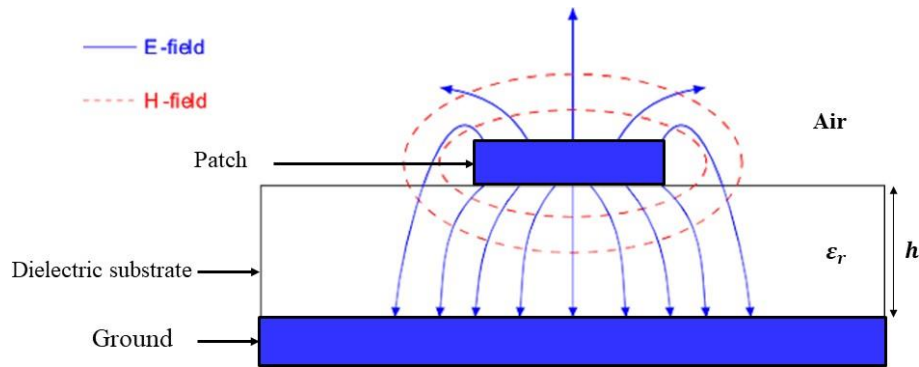


Figure 1.3 Fringing fields in patch antennas [5].

1.2.4 Microstrip Antenna Feeding Methods

Feeding the microstrip antenna is very important to improve the antenna input impedance matching. The feeding techniques used in the patch antenna are divided into two important classes [6].

1.2.4.1 Contacting feed

In this method, the power is directly fed to the radiating element. The most commonly used methods of this class are Microstrip and Coaxial Feed line.

a. Microstrip Line Feed

In this type of feed technique, a conducting strip is connected directly to the microstrip patch's edge, as shown in figure 2. The conducting strip is smaller in width than the patch, and this kind of feed arrangement has the advantage that the feed can be etched on the same substrate to provide a planar structure [6].

b. Co-axial Feed

The co-axial feed is a non-planar feeding technique in which a co-axial cable is used to feed the patch. The inner conductor of the co-axial connector extends through the dielectric, making a metal contact with the patch, and the outer conductor of the cable is connected to the ground plane

The inner conductor extends through the dielectric and is soldered to the patch, while the outer conductor of the coaxial connector is connected to the ground plane as shown in figure 1.5. To obtain better input impedance matching the feed line position can be altered to any desired location on the patch [7].

1.2.4.2 Non-Contacting Feed

The power is not fed directly to the patch but is instead transferred from the feed line through electromagnetic coupling. This is done using Aperture or Proximity Coupled Feed [7].

a. Aperture Coupled Feed

A microstrip feed line printed on the lower substrate is electromagnetically coupled to the patch through a slot printed in the common ground plane [7].

b. Proximity Coupled Feed

In this feeding mechanism, two dielectric substrates are used and the feed line is between the two substrates. The radiating patch is on top of the upper substrate. This feed technique eliminates spurious feed radiation and provides very high bandwidth due to the increase in the thickness of the microstrip patch antenna [7].

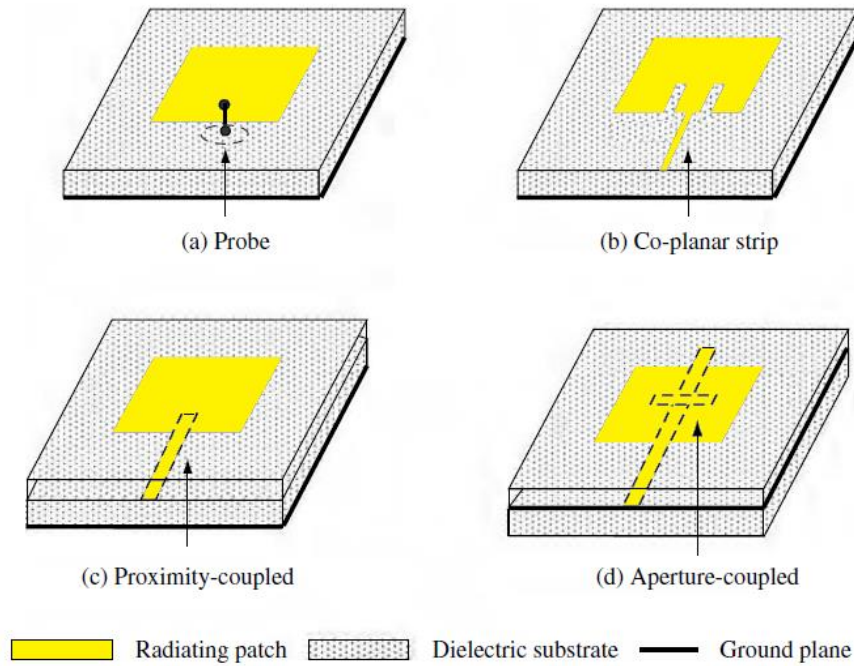


Figure 1.4 Four common feeding methods of microstrip patch antenna.

Table 1.1 shows a comparison between the different feeding techniques mentioned in the previous unit.

Table1.1: Comparison between different patch antenna feeding techniques [10].

Characteristic	Microstrip line feed	Coaxial probe feed	Aperture coupled feed	Proximity coupled feed
Spurious feed radiation	More	More	less	minimum
Impedance matching	Easy	Easy	easy	easy
Reliability	Better	Poor	Good	Good
Bandwidth	2 - 5%	2 - 5%	2 - 5%	2 - 5%

1.2.5 Method Analysis

Methods of analysis the most well-known method for the analysis of microstrip patch antenna are divided into two groups of methods:

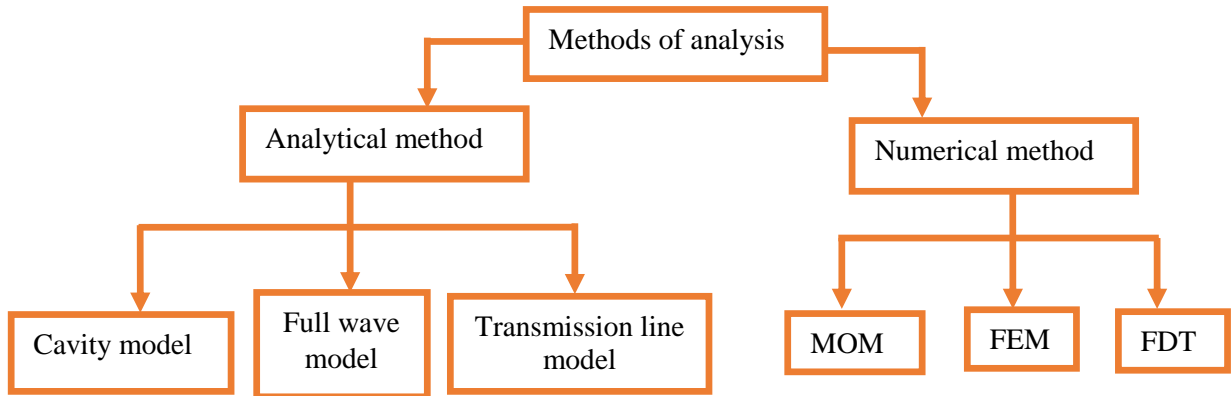


Figure 1.5 Method Analysis

1.2.6 Antenna Parameters

1.2.6.1 Input Impedance

It is the impedance offered by the antenna at its terminals. It can be also defined as “the ratio of the voltage to the current across the input terminals” or “the ratio of the appropriate components of the electric to magnetic fields at a point [13]. It is defined as:

$$Z_{in} = Z_0 \frac{1+\Gamma}{1-\Gamma} \quad (1-1)$$

Where

- Z_0 is the characteristic impedance
- Γ is input reflection coefficient.

1.2.6.2 Directivity

Directivity is the increase in power density in a given direction at a fixed distance from the antenna, relative to the power density averaged over all directions. Usually, the maximum value of directivity is of primary interest, and here we use directivity to mean maximum directivity. Hence, directivity is a measure of the increase in maximum power density at a fixed distance compared to that from a hypothetical isotropic radiator. Directivity, D , is a unit-less power ratio, usually expressed in dB [14].

$$D(\theta, \varphi) = 4\pi \frac{U(\theta, \varphi)}{P_{rad}} \quad (1-2)$$

Where $D(\theta, \varphi)$ is the antenna directivity, $U(\theta, \varphi)$ is the radiation intensity and P_{rad} is the total radiated power.

1.2.6.3 Efficiency

The total antenna efficiency is used to take into account losses within the antenna and at the input terminals. These losses occur due to the mismatch between the antenna and transmission line which causes reflections and the conductor and dielectric losses [15]. The total efficiency is given by the equation:

$$e_0 = e_r e_c e_d \quad (1-3)$$

Where

- e_0 is the total efficiency,
- e_r is the reflection (mismatch) efficiency,
- e_c is the conductor efficiency
- e_d is the dielectric efficiency.

1.2.6.4 Gain

Antenna gain is closely related to the directivity, but it also takes into account the efficiency of the antenna. The gain of an antenna in a given direction is defined as the ratio of the intensity, in a given direction, and the radiation intensity that would be obtained if the power accepted by the antenna were radiated isotopically. This is called the absolute gain. The radiation intensity corresponding to the isotopically radiated power is equal to the power input by the antenna divided by 4π . Thus,

$$G(\phi, \theta) = 4\pi \frac{U(\phi, \theta)}{P_{in}} \quad (1-4)$$

where G is the gain. P_{in} is the total input power and U is the radiation intensity. In many applications, partial gains G_ϕ and G_θ are used. These partial gains are defined as:

$$G_\phi = 4\pi \frac{U_\phi}{P_{in}} \quad (1-5)$$

$$G_\theta = 4\pi \frac{U_\theta}{P_{in}} \quad (1-6)$$

Where U_ϕ is the radiation intensity in a given direction contained in the ϕ -field component, U_θ is the radiation intensity in a given direction contained in the θ -field component.

The realized gain of an antenna is calculated by considering the total efficiency of the antenna, along with its directivity. In a simple way, the realized gain is what you actually get with the actual mismatch. It takes into account total antenna efficiency not radiation efficiency.

1.2.6.5 Radiation Pattern

The antenna radiation pattern is defined as a mathematical function or graphical representation of the radiation properties of the antenna as a function of the space parameters. This pattern is usually determined in the far field region. It has various properties such as power flux density, radiation intensity, field strength, directivity phase or polarization. The performance of the antenna is often described in terms of its principal E- and H- plane patterns [8].

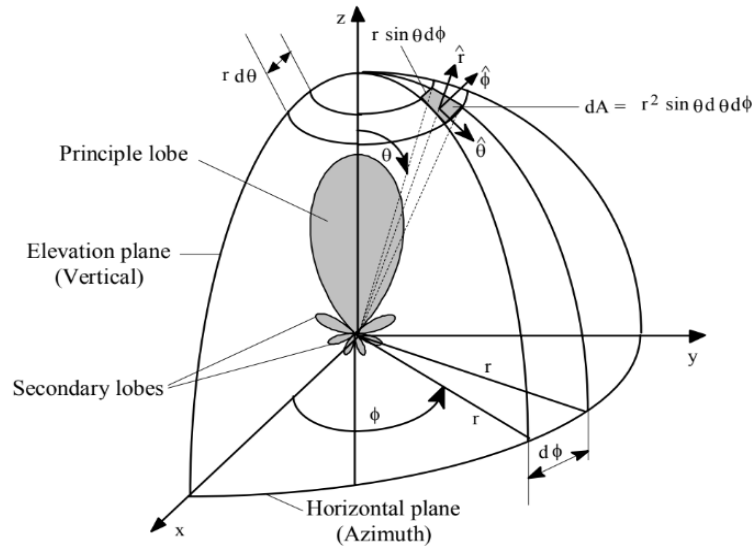


Figure 1.6 Radiation pattern in spherical coordinates [8].

1.2.7 Advantages and disadvantages of Microstrip antenna

Microstrip antenna has several advantages compared to other microwave antennas, some advantages are:

- Light weight and low volume.
- Low profile planar configuration which can be easily made conformal to host surface.
- Low fabrication cost, hence can be manufactured in large quantities.
- Supports both, linear as well as circular polarization.
- Can be easily integrated with microwave integrated circuits (MICs).
- Capable of dual and triple frequency operations.
- Mechanically robust when mounted on rigid surfaces.

Microstrip antenna has also some disadvantages compared to conventional microwave antennas they are some:

- Narrow bandwidth.
- Low efficiency.
- Low Gain.
- Low power handling capacity.
- Extraneous radiation from feeds and junctions.
- Surface wave excitation.

1.3 Introduction to Multiple Input Multiple Output Systems (MIMO)

1.3.1 introduction

MIMO technology combats multipath fading in wireless channels by sending the data from multiple antennas at the transmitter to multiple receivers at the receiver. The data from multiple antennas go through different paths in the wireless environment, and thus the chance of receiving a good representation of the transmitted data in such fading environments increases, achieving better data rates when sending parallel streams of different data from each transmitting antenna [9]. MIMO system improves the communication performance by utilizing multiple antennas at both the transmitter and receiver ends. The communication range and throughout of the communication system is increased significantly using MIMO. to describe the performance of antenna there are several commonly used antenna parameters, including impedance bandwidth, radiation pattern, directivity, gain, and polarization [10].

1.3.2 Techniques of isolation

1.3.2.a Frequency diversity

In frequency diversity technique, we will send information bearing signals by carriers whose frequency gap is greater than coherence bandwidth of the channel; for instance, frequency hopped spread spectrum system [11].

1.3.2.b Time diversity

In time diversity technique, we will send information bearing signals in different time slots which is greater than coherence time of the channel: for example, channel coding with interleaving end [11].

1.3.2.c Space diversity

In space diversity technique, we employ multiple antennas, which are placed amply far away, at the transmitter and receiver [11].

1.3.3 Mutual Coupling

Despite many advantages, the MIMO antenna system suffers from a serious problem caused by strong mutual coupling between antenna elements, which cause signal interference between them and a higher value of mutual coupling lowers antenna efficiency, so that, in general, 0.5λ or more distance between antennas is needed to avoid the degradation of antenna performance. As is common in cellular phone handsets, higher levels of mutual coupling, which can easily occur in a handset, these systems can significantly degrade antenna efficiencies and produce an undesirable signal correlation between multiple antenna outputs. High signal correlation is associated with the loss of spectral efficiency and can degrade system throughput and battery efficiency. To achieve the desired low signal correlation, these communication systems require high diversity and reduced coupling, which is also identified as a high port-to-port isolation [11].

1.3.4 MIMO Application

1.3.4.a Data Rate Extension

MIMO with low bandwidth and high spectral efficiency solves the problem of high speed and low speed users. In MIMO 1 Gbps data rate is achieved with 20 MHz bandwidth only. MIMO with different modulation like binary phase shift keying (BPSK), quadrature phase shift keying (QPSK), and quadrature amplitude modulation (QAM), offers variable data rates [16].

1.3.4.b Power Saving

Unlike other systems like SISO, MIMO does not consume much power. Therefore, it is suitable for wireless applications [16].

1.3.4.c Capacity Enhancement

Capacity of MIMO is very high and is not dependent completely on the bandwidth.

References

- [1] The McGraw-Hill Companies 2007 under license agreement with Books24x7
- [2] Punit S. Nakar. Design of a compact microstrip patch antenna for use in wireless/cellular devices. Master's thesis, The Florida State University, 2004.
- [3] Balanis, C. A. (2005). Antenna Theory Analysis and Design Third Edition. New Jersey: John Wiley & Sons, Inc.
- [4]
- [5]
- [6] ParwinderKaur, "Gain Enhancement of Microstrip Patch Antenna with Slotting Techniques" International Journal Of Advanced Research in Engineering & Management (IJAREM)- Volume 03, issue 01, PP.13-19, ISSN:2456-2033, Feb 2017
- [7] A. S. Mohammed, A, R Yauri and A. Kabir, " Review of feeding technique for microstrip patch antenna " International jornal of computer application, vol. 178, pp. 97-887, 2019
- [8] C. A Balanis, antenna theory: analysis and design: jhon wiley & sons, 2015
- [9] Ramesh Garg, Prakash Bhartia, Inder J Bahl, and Apisak Ittipiboon. Microstrip antenna design handbook. Artech house, 2001.
- [14] Malviya, L., Panigrahi, R. K., & Kartikeyan, M. V. Mimo antennas for Wireless Communication: Theory and Design. CRC Press, 2021.
- [10] J Kshetrimayum. Fundamentals of Mimo Wireless Communications. Cambridge University Press, 2017.
- [11] Malviya, L., Panigrahi, R. K., & Kartikeyan, M. V. Mimo antennas for Wireless Communication: Theory and Design. CRC Press, 2021.

Chapter 2

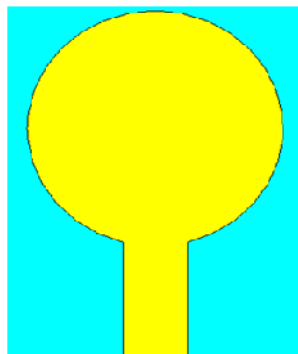
A compact quad bands spiral monopole antenna for WiMAW/WLAN and C applications

1. Introduction

Compact antennas with characteristics of multiband operations are the requirement of wireless communication systems. Microstrip antennas are very attractive candidates suitable for wireless devices due to their unique characteristics such as low-profile, light weight, ease of integration.

In this chapter, we propose a DMS technique for miniaturization quad band microstrip patch antenna for WiMAX and C band applications. A CST Microwave Studio (CST MWS) is used to model the designed antenna.

2. Antenna Desgin



Ant-A

Figure 2.1.1: Evolution steps Ant-A

The form of the reference antenna is selected as circular patch (Ant-A) as depicted in Figure 2.1.1 The antenna operates at resonant frequency 4.3GHz with wideband characteristic as presented in Figure 2.1.1.1

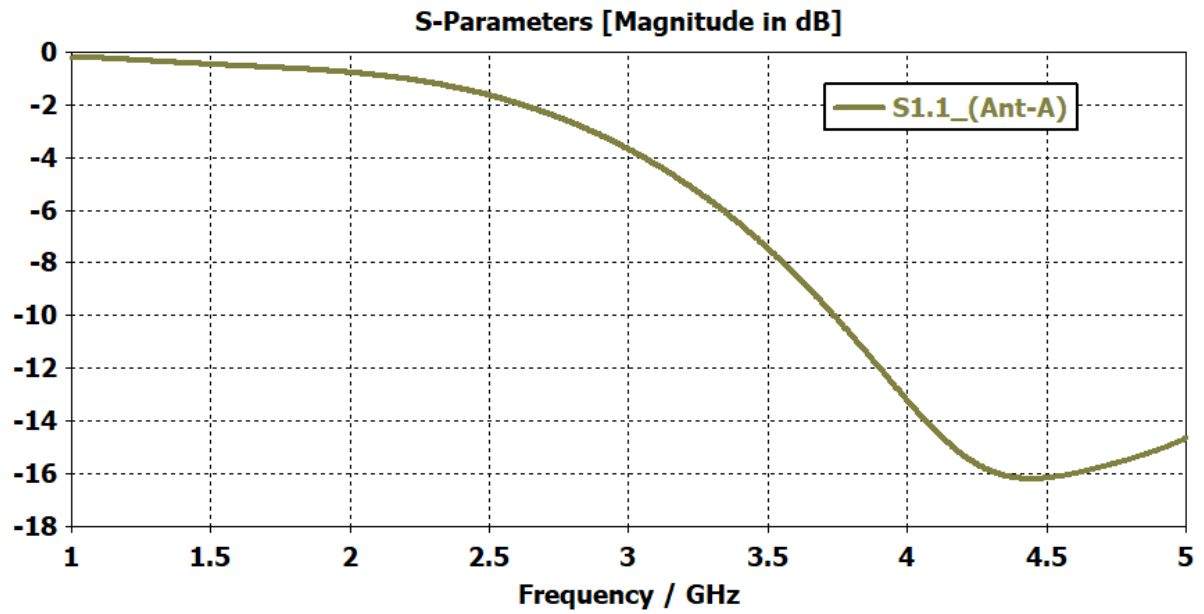
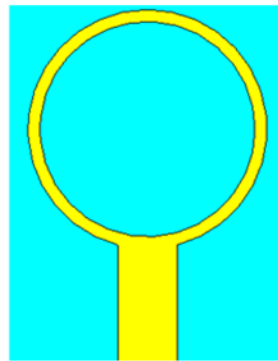


Figure 2.1.1.1: Simulated input reflection coefficient Ant-A.



Ant-B

Figure 2.1.2: Evolution steps Ant-B

a circular ring is derived as Ant-B to shift the operating frequency to 4GHz with a reflection coefficient (S11) of -24 dB as we can see in Figure 2.1.2.1

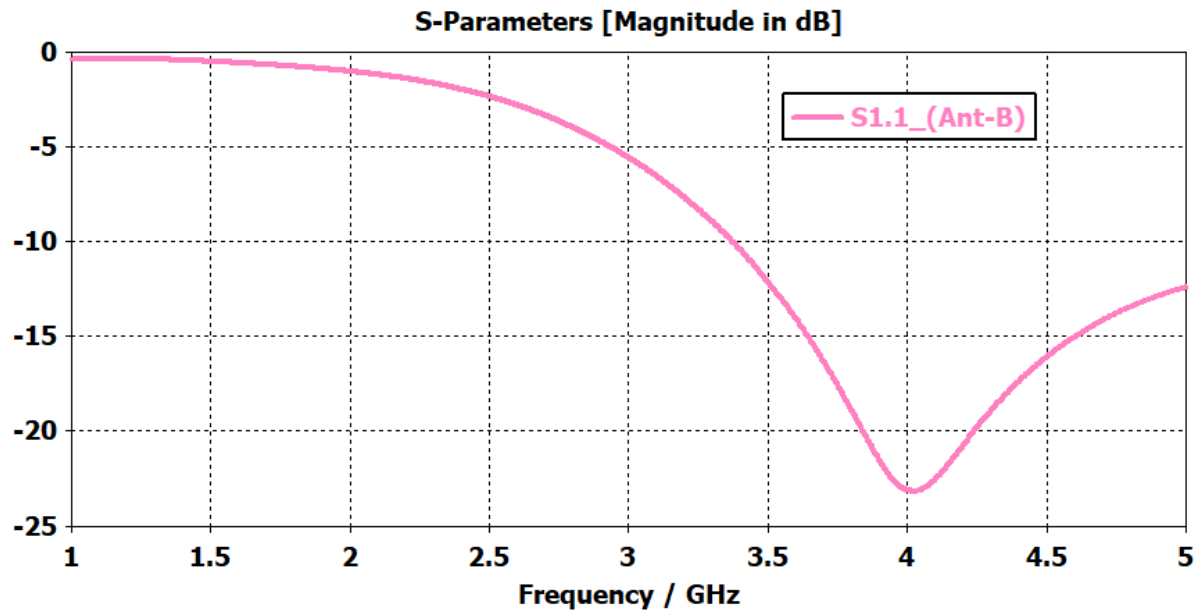
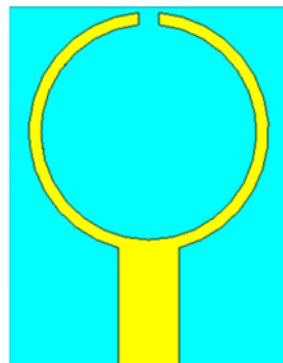


Figure 2.1.2.1: Simulated input reflection coefficient Ant-B.



Ant-C

Figure 2.1.3: Evolution steps Ant-C

In Ant-C a slot is added to ring to get a C-shape, from Figure 2.3 in the case of Ant-C the impedance is improved and S11 level is reached to -43dB as we can see in Figure 2.3.3.1

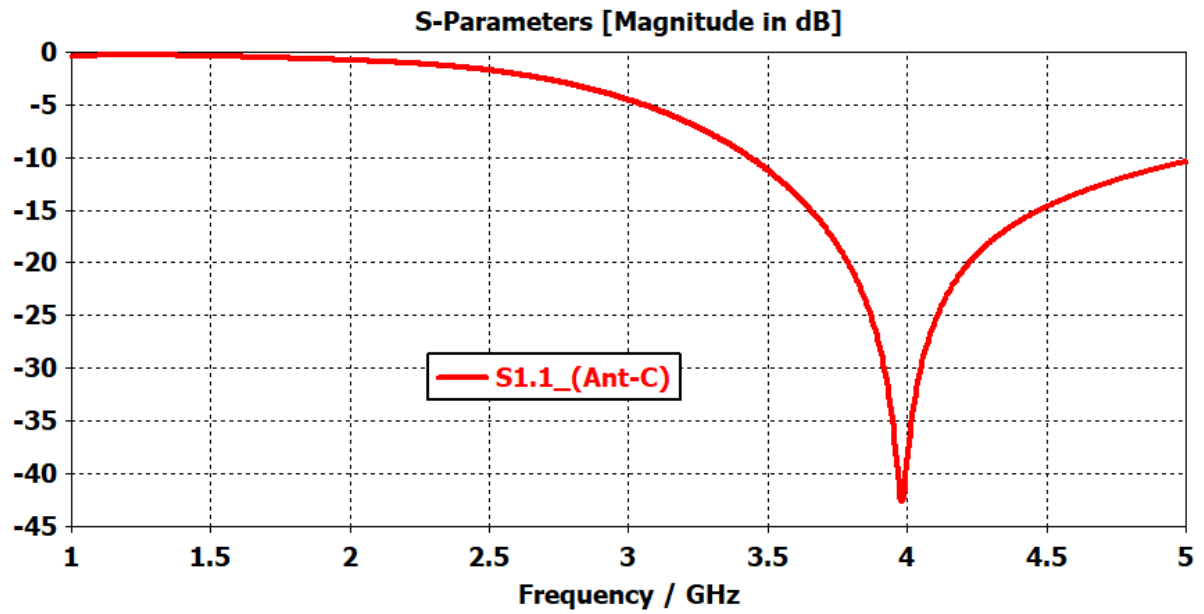
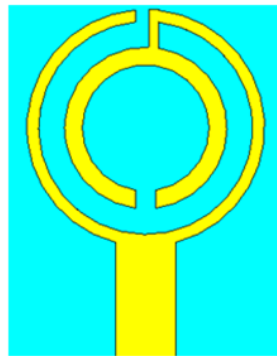


Figure 2.1.3.1: Simulated input reflection coefficient Ant-C



Ant-D

Figure 2.1.4: Evolution steps Ant-D

An inverted C-shape is also introduced to our design as Ant-D (Figure 2.2.4) to get a tri-band at 1.48GHz, 3.4GHz and 4.35GHz as illustrated in Figure 2.3.4.1

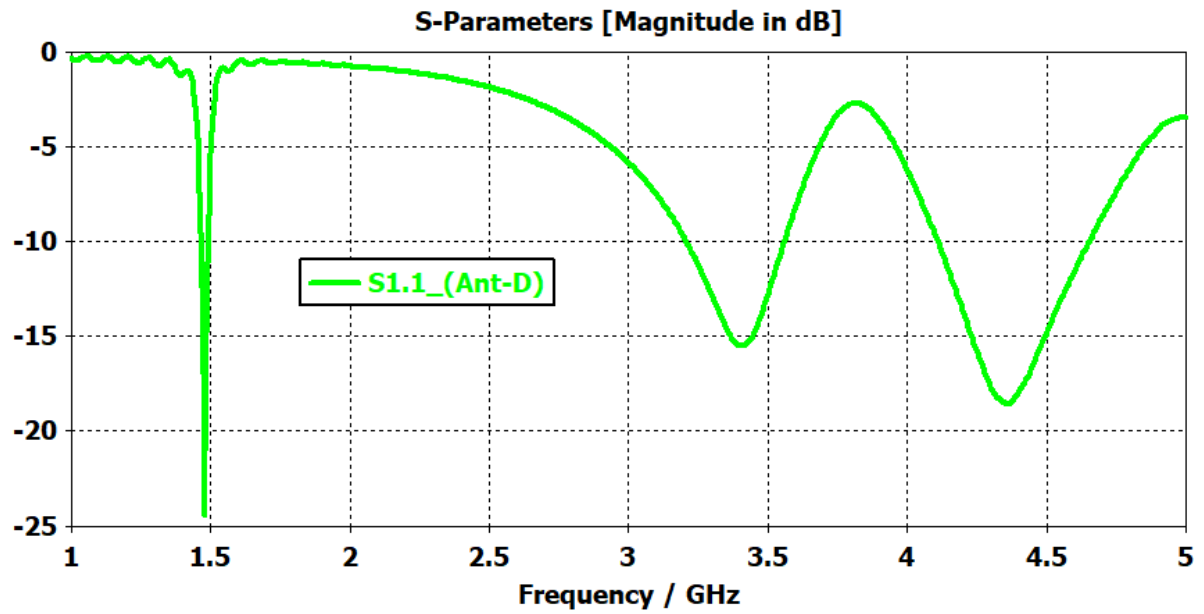
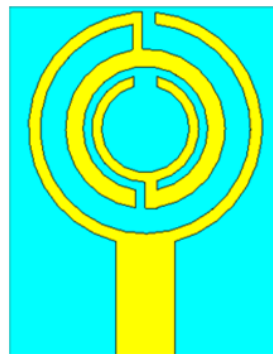


Figure 2.3.4.1: Simulated input reflection coefficient Ant-D



Ant-E

Figure 2.1.5: Evolution steps Ant-E

To achieve a tri-band WiMAX application another C-shape with small size is introduced to our design as depicted in Figure 2.1.5 (Ant-E). The insertion of C-shape the resonant frequencies is shifted to lower bands to reach (1.36), (2.45) and 3.63GHz as illustrated in Figure 2.1.5.1

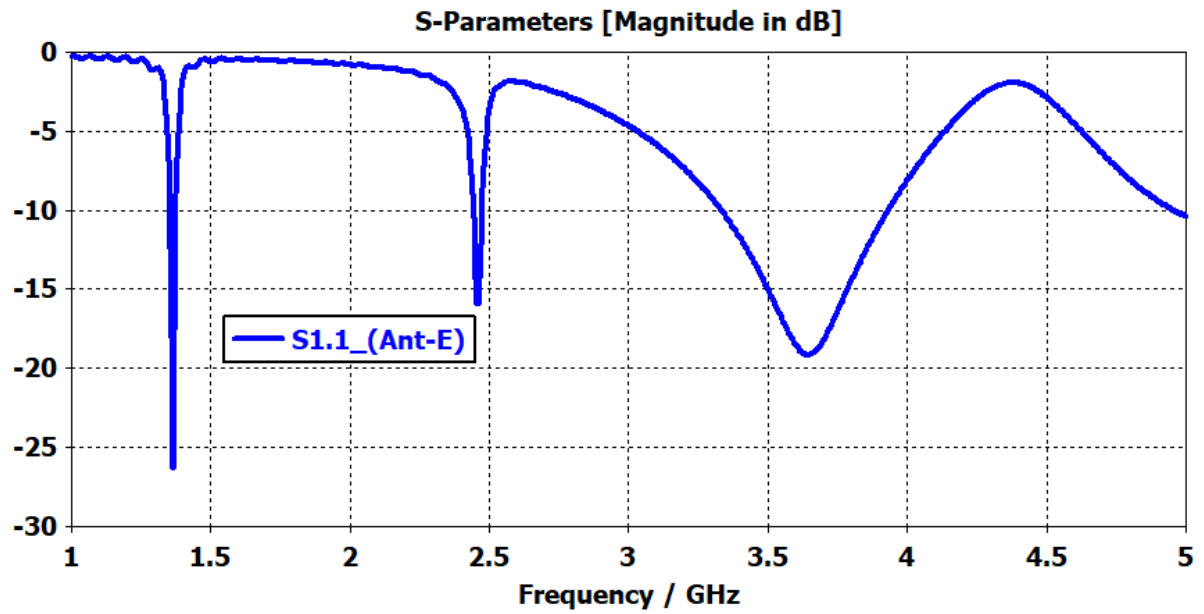
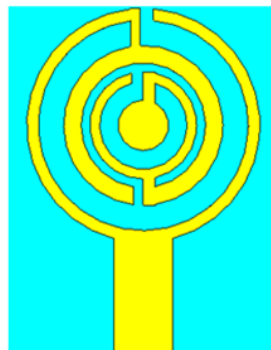


Figure 2.1.5.1: Simulated input reflection coefficient Ant-E.



Ant-F

Figure 2.1.6: Evolution steps Ant-F

Finally, to get quad band a small circular shape is introduced in the center of the proposed structure (Ant-F). Figure 2.1.6 shows that by inserting a small circular shape another resonant frequency is created at 4.15GHz in C-band application.

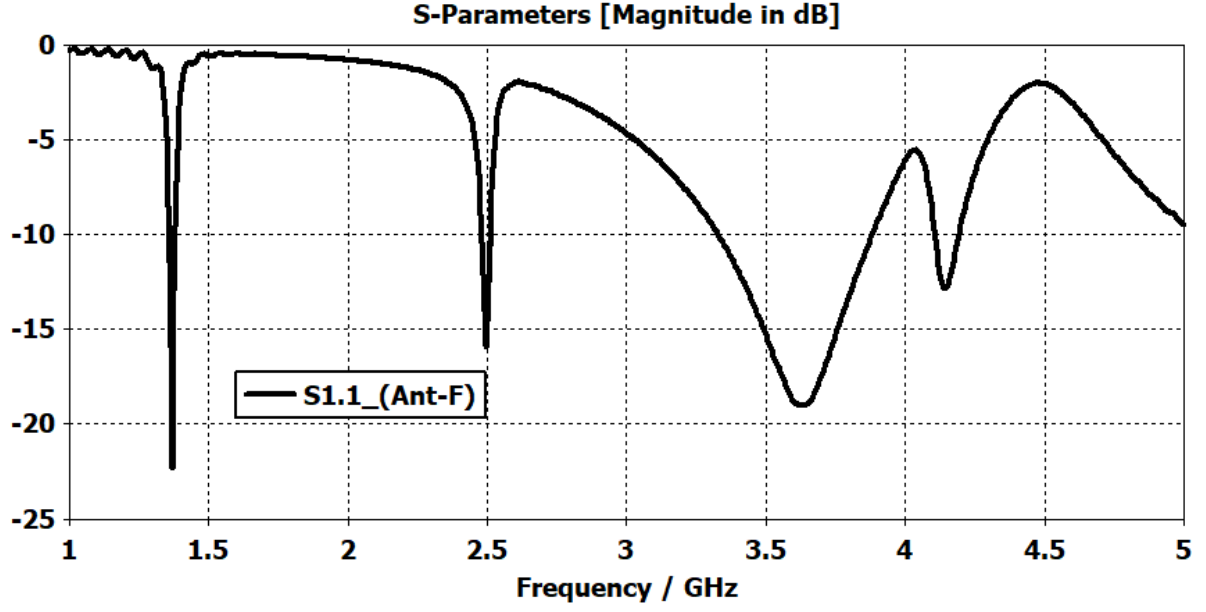


Figure 2.1.6.1: Simulated input reflection coefficient Ant-F

The configuration of the proposed compact quad-band spiral antenna for WiMAX and C applications is presented in Figure 2.1. The proposed structure comprises of new shape of spiral which is inspired from literature [1, 2] and it is fed by a microstrip feed line. The antenna is printed on an FR-4 substrate of thickness $h = 1.6$ mm, loss tangent $\tan \delta = 0.02$ and dielectric constant $\epsilon_r = 4.3$. The complete physical size of the proposed antenna is $14 \times 18 \times 1.62$ mm³.

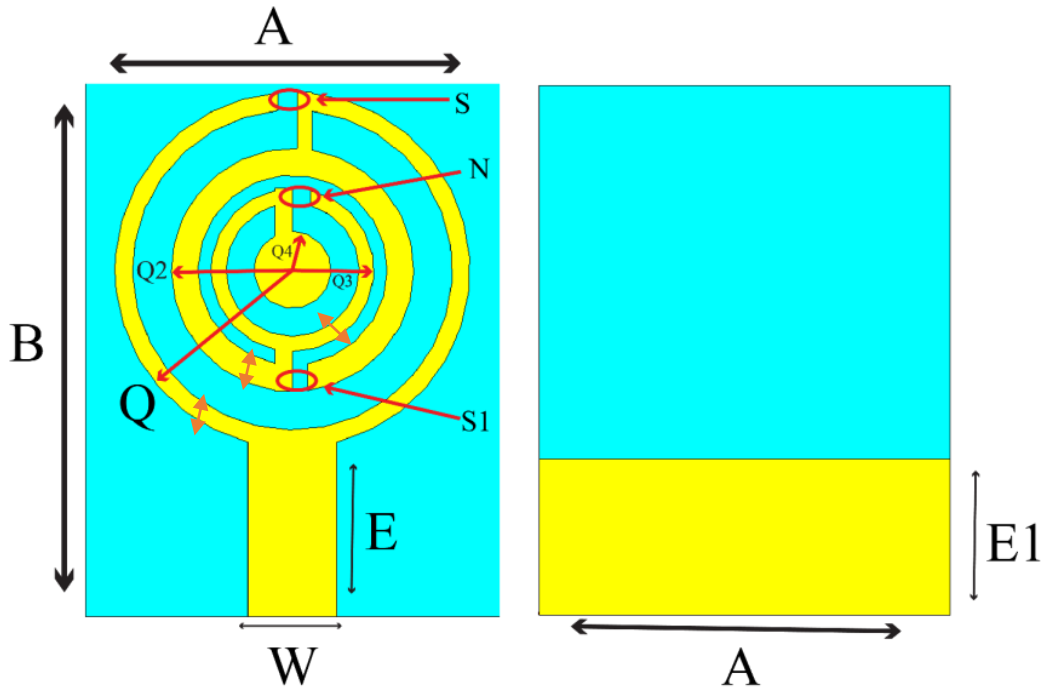


Figure 2.1: Geometry of the proposed antenna. Top and Bottom view.

The geometry of the final proposed antenna is shown in Figure 2.1. The optimized final dimensions of the proposed antenna are given in Table 2.1. The simulated input reflection coefficient of the proposed structure is depicted in Figure 2.4. From the plot, the antenna exhibits four bands at 1.63, 2.5, 3.63 and 4.15 GHz respectively.

Table 2.1 : Detailed parameters antenna.

Parameter	A	B	E	W	Q	Q2	Q3	Q4	E1	S	S1	N	R	R2	R3
Value(mm)	14	18	6.0	3.0	6.0	4.1	2.75	1.3	5.3	1.0	1.0	1.2			

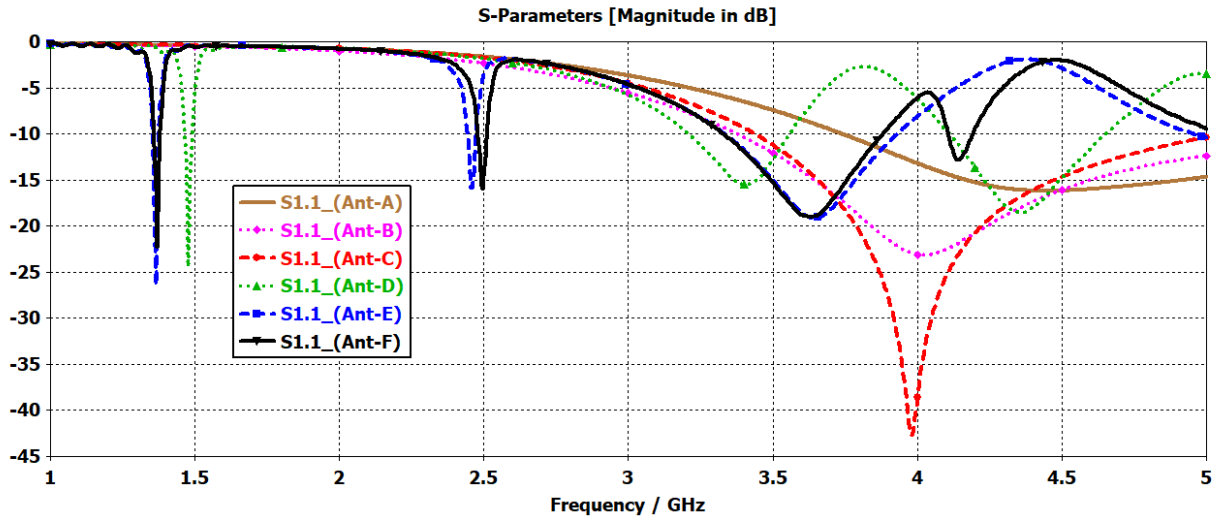


Figure 2.3: Simulated input reflection coefficient of different stages of the proposed antenna.

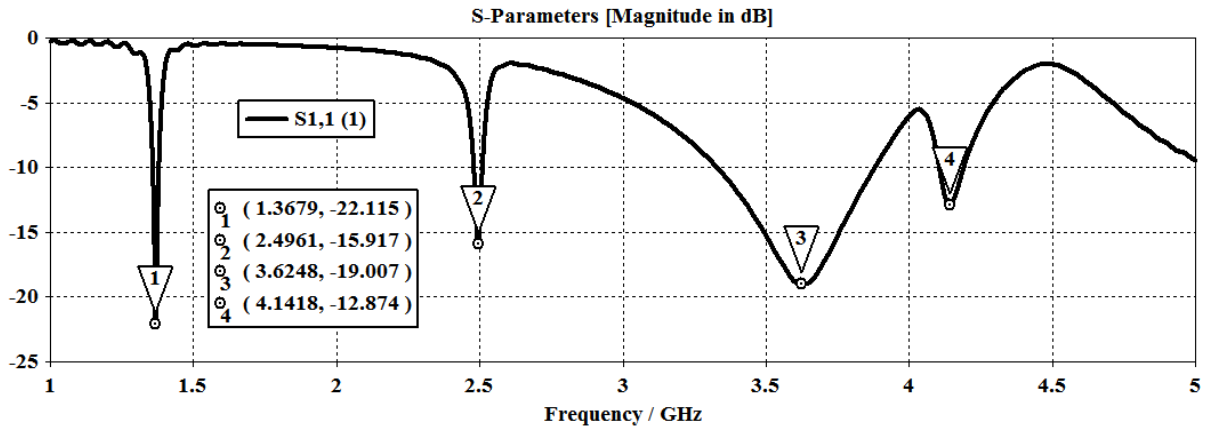


Figure 2.4: Simulated the input reflection coefficient of the final structure.

2.2.1 Parametric study

To further investigate the proposed antenna performance, a parametric study is carried out and discussed.

- **Effect of Q**

Figure 2.5 shows the input reflection coefficient for different values of Q whereas the other parameters are kept constants. From the graph, it is clear that as Q is decreasing the third frequency is shifted towards the higher frequencies with small effects in the second and fourth frequencies this is due to mutual coupling between the C-shapes.

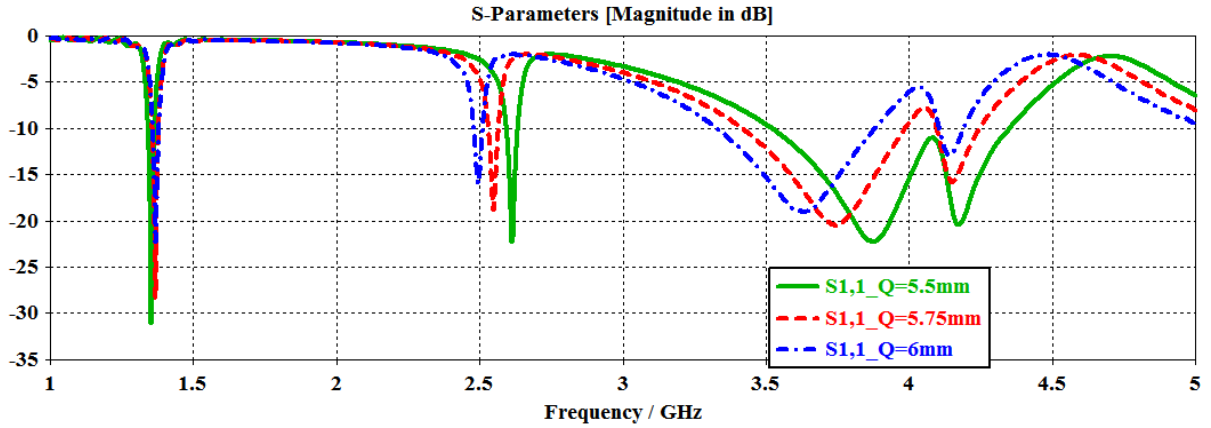


Figure 2.5: Simulated input reflection coefficient for various Q

- **Effect of Q1**

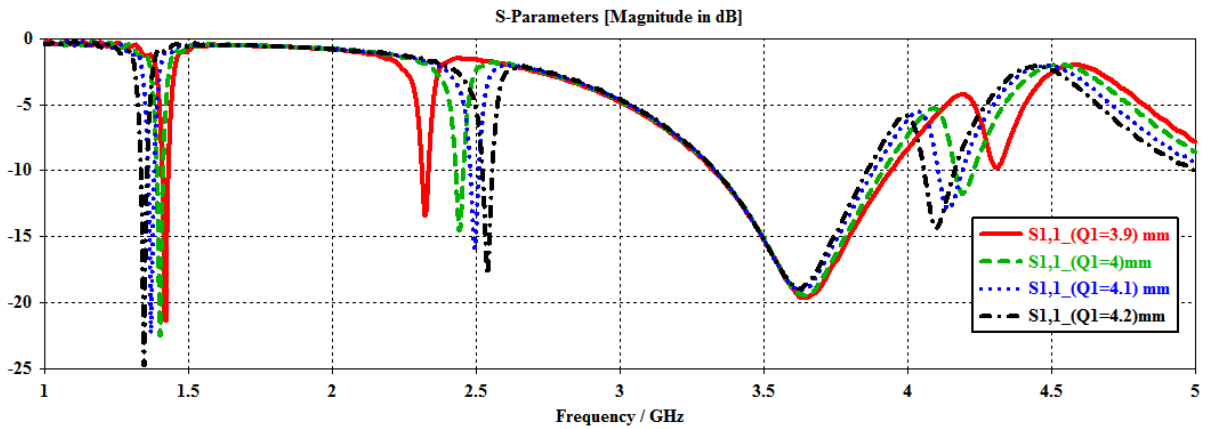


Figure 2.6: Simulated input reflection coefficient for different values Q1

Figure 2.6 shows the input reflection coefficient for different values of Q1 (second C-shape) with other parameters are kept constants. From the plot, it is observed that as increasing Q1 the second frequency is shifted towards higher values side while the first and the fourth bands decrease significantly. For Q1 equals to 4.1 mm, the three resonant frequencies are tuned to the desired bands.

- **Effect of Q3**

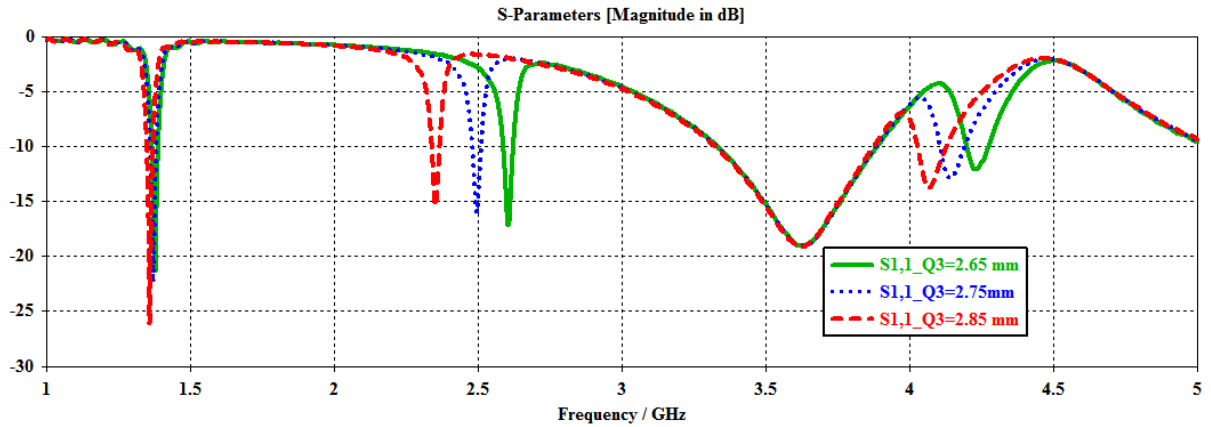


Figure 2.7: Effect of Q3 on the (S11)

Figure 2.7 displays the antenna input reflection coefficient for diverse values of the third ring Q3

. It is seen that by increasing Q3, the second resonant frequency decreases while the upper resonance increases slightly. For Q3 equal 2.75mm, the two bands are centered at the desired frequencies.

- **Effect of Q4**

The effect of changing the parameter Q4 on the antenna input reflection coefficient characteristics is depicted in Figure 2.8. It can be observed from the Figure that by increasing the value of Q4, the cut off frequency of the fourth band is shifted towards lower frequency. Hence, it can be concluded that good results are obtained for Q4=1.3mm.

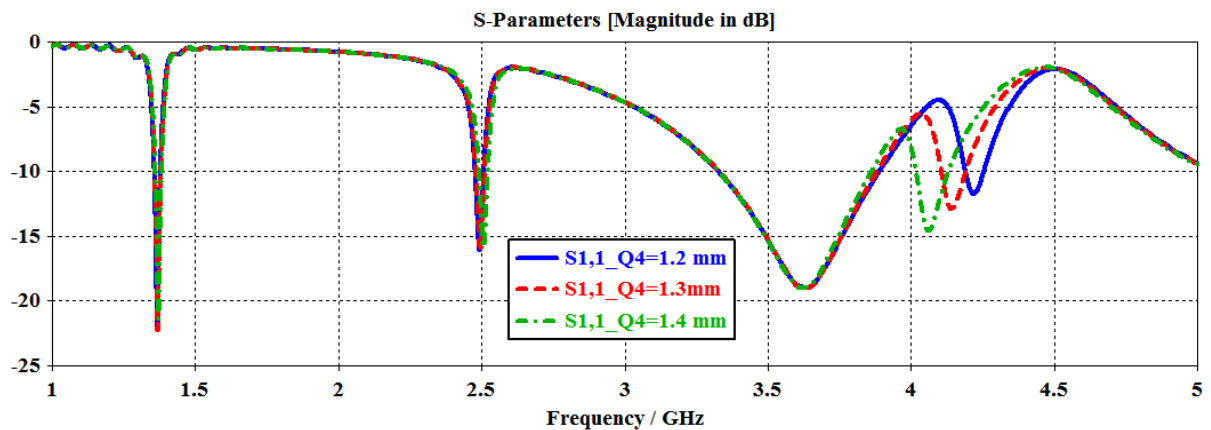


Figure 2.8 : Effect of Q4 on the S(11)

2.2.2 Current Distribution

The working mechanism of the proposed antenna could be defined with the help of the revealed current distribution. The current distribution of the proposed antenna at each resonant frequency is shown in Figure 2.9.

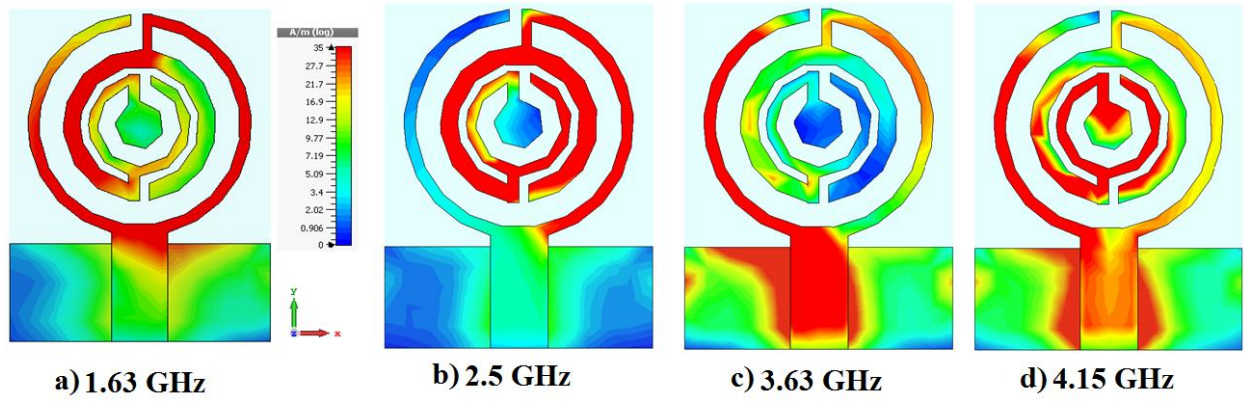
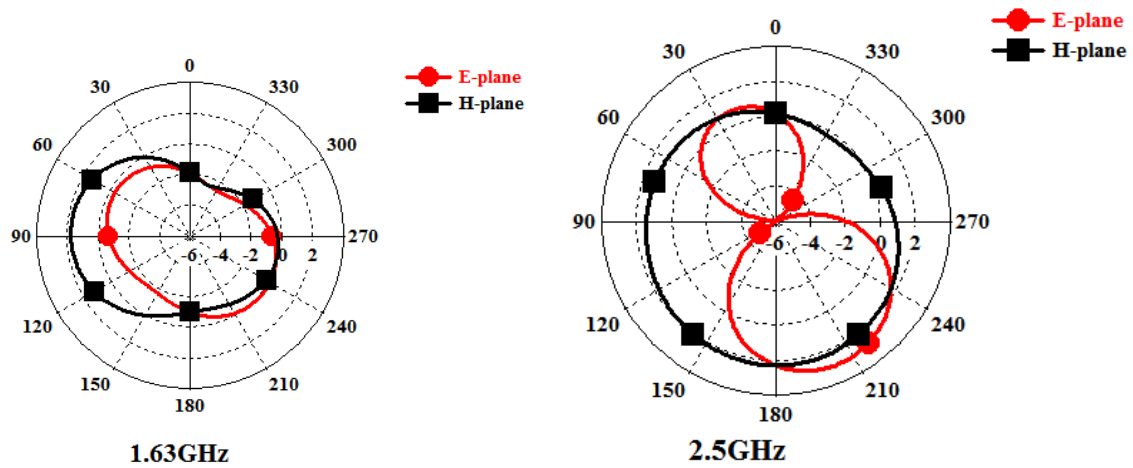


Figure 2.9: Surface current distribution of the proposed antenna at (a) 1.36 GHz, (b) 2.5 GHz, (c) 3.63 GHz and (c) 4.15 GHz.

From the graph, it is inferred that the current is concentrated along the outer ring and the half surface of the second ring for 1.63GHz. At the second ring the current is more strong at the second ring and the half surface of outer and inner rings this is due mutual coupling between the rings. For resonant at 3.63GHz, the current is maximum at the outer ring whereas for 4.15GHz the current is maximum in small circle.



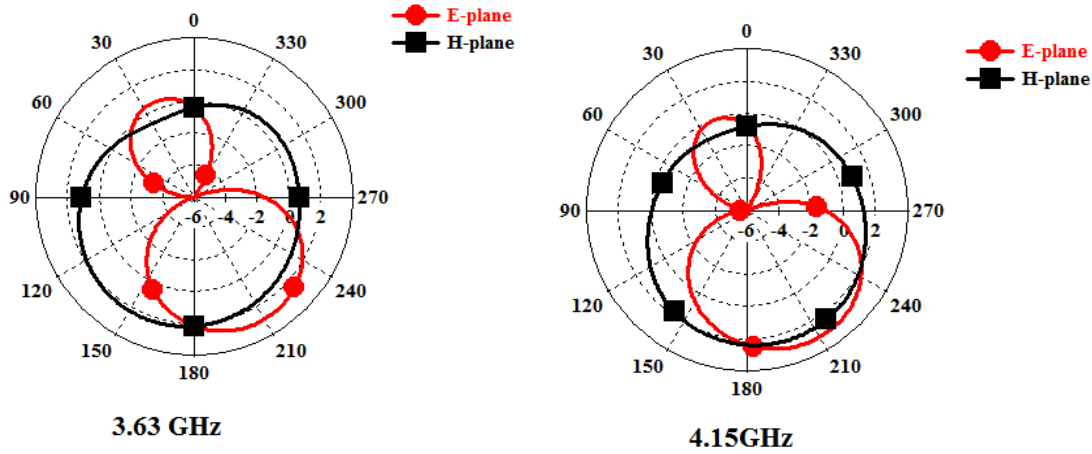


Figure 2.10: Simulated radiation patterns of the proposed quad-band antenna.

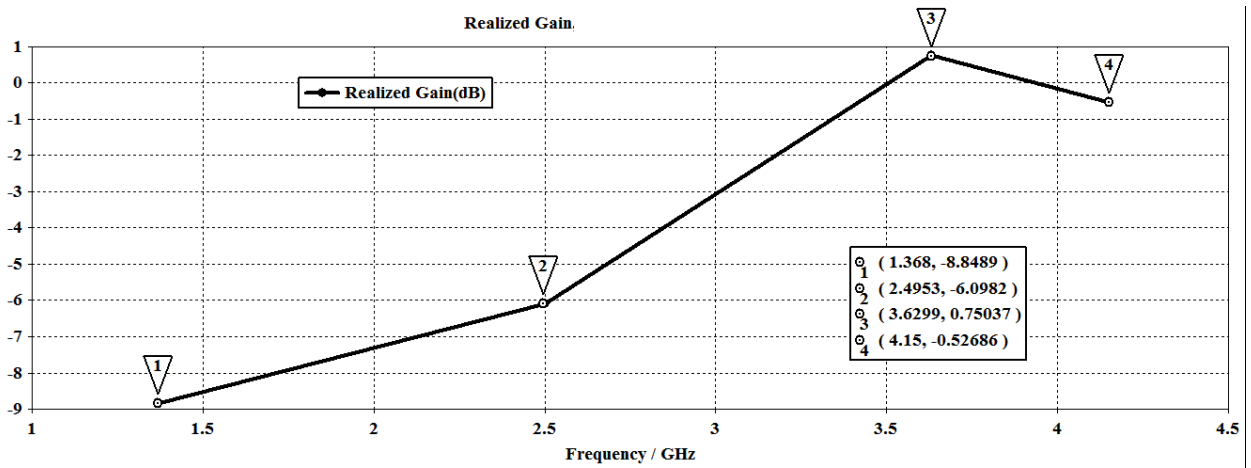


Figure 2.11: The simulated gain at four band frequencies of the proposed design

The radiation pattern of the antenna at the four operating frequencies 1.63GHz, 2.5GHz , 3.63GHz and 4.15GHz GHz are presented in Figure 2.10. it is observed that the proposed antenna shows a dipole-like patterns in the E-plane (yoz) whereas in the H-plane (xoz) , an omnidirectional radiation pattern in characteristics is achieved for all resonant frequencies. The simulated gain of the antenna are shown in Figure 2.11 with max gain is 0.75dB .

2.3 Fabrication and measurements

Photographs of the top and bottom views of the fabricated antenna are shown in Figures 2.12. The return loss characteristic of the antenna is measured by using vector network analyser and the simulated and measured return losses results of the antenna are illustrated in Figure 2.13. It can be observed that the simulated and measured results are in good agreement, showing a quad-band operation with measured 10-dB impedance bandwidths of 40 MHz (1.33 – 1.37 GHz), 30 MHz (2.50-

2.53 GHz), 450 MHz (3.34 – 3.85 GHz) and 70 MHz (4.08 – 4.15 GHz), covering several communication bands such as WiMAX and C-band.

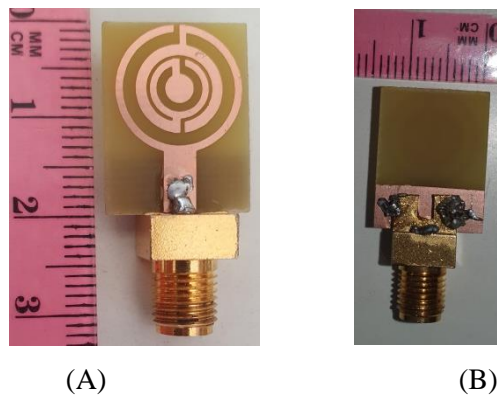
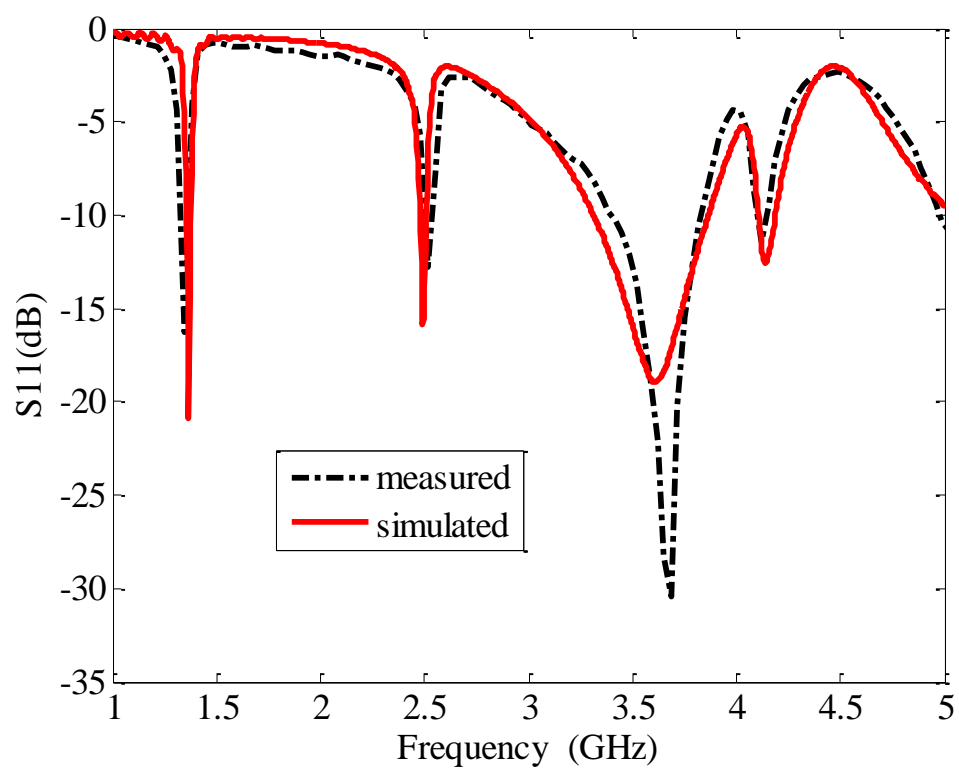
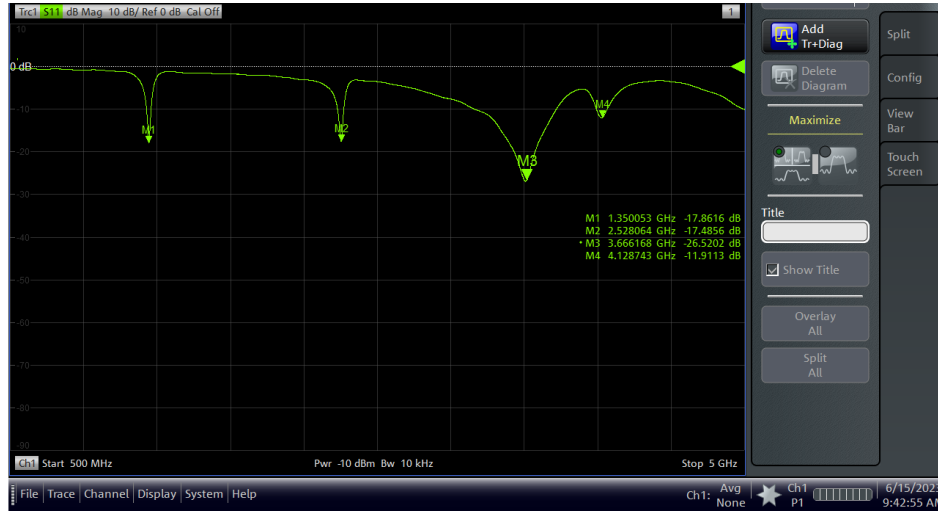


Figure 2.12: Fabricated prototype of designed antenna (A) front view (B) back view



(A)



(B)

Figure 2.13: Measured and simulated input reflection coefficient

The comparison of the suggested antenna with the recent implementations in various research works is shown in Table 2.2. It is observed that the proposed antenna exhibits compactness and multiband incorporated.

Table 2.2: Comparison of our antenna with the existing antennas.

Ref.	Substrate	Size(mm ²)	Concept	Working bands(GHz)	bands
[2]	FR4	25 × 31.7	SRR and NBCSRR	3.45 , 4.18 and 5.10	Tri-band
[3]	//	40× 40	DMS	2.4,3.5,4.9	//
[4]	//	27× 27	Spiral strip – DMS	0.9/2.4/3.5/5.8	Quad band
[5]	//	37 × 28	Fractal	2.07/3.73/4.76	Tri-band
This work	//	14 × 18	DMS	1.63/2.5/3.63/4.15	

References

- [1] S. Bhattacharjee, S. Maity, S. R. Bhadra Chaudhuri, and M. Mitra, "Metamaterial-inspired wideband biocompatible antenna for implantable applications," *IET Microwaves, Antennas & Propagation*, vol. 12, pp. 1799-1805, 2018.
- [2] R. Pandeewari, "SRR and NBCSRR inspired CPW fed triple band antenna with modified ground plane," *Progress In Electromagnetics Research C*, vol. 80, pp. 111-118, 2018.
- [3] K. Kumari, R. K. Jaiswal, and K. V. Srivastava, "A compact triple band circularly polarized planar antenna for wireless application," *Microwave and Optical Technology Letters*, vol. 62, pp. 2611-2617, 2020.
- [4] A. A. Jabar and D. K. Naji, "Design of miniaturized quad-band dual-arm spiral patch antenna for RFID, WLAN and WiMAX applications," *Progress In Electromagnetics Research C*, vol. 91, pp. 97-113, 2019.
- [5] S. Nallapaneni and P. Muthusamy, "Design of multiband fractal antenna loaded with parasitic elements for gain enhancement," *International Journal of RF and Microwave Computer-Aided Engineering*, vol. 31, p. e22622, 2021.

Chapter 3

Compact quad band MIMO antenna for WiMAX and C applications

3.1 Introductions

In this chapter, a compact quad band MIMO antenna is presented. The antenna element is the same as the antenna that is discussed in chapter 2. In order to minimize the overall size of the MIMO antenna with high isolation, an inverted L-shaped bar is inserted between the antenna elements. The proposed design printed on an FR-4 substrate with dielectric constant 4.3, a thickness of 1.62 mm and a loss tangent of 0.02. A detailed study of the proposed compact MIMO antenna will be presented.

3.2 DESIGN OF MIMO ANTENNA

The geometry of the proposed quad band MIMO antenna for WiMAX and C band applications is shown in Figure 3.1. The design involves two identical planar monopole elements placed orthogonally to each other (angle 90°) and constructed on the top side of the dielectric substrate and backed by the partial ground. The radiators are the same as the single quad band spiral monopole antenna that is discussed in chapter 2. The suggested quad band MIMO antenna is printed over FR-4 substrate with dielectric constant 4.3, a thickness of 1.6 mm and a loss tangent of 0.02. The overall size of the proposed structure is $18 \times 36 \times 1.6 \text{ mm}^3$.

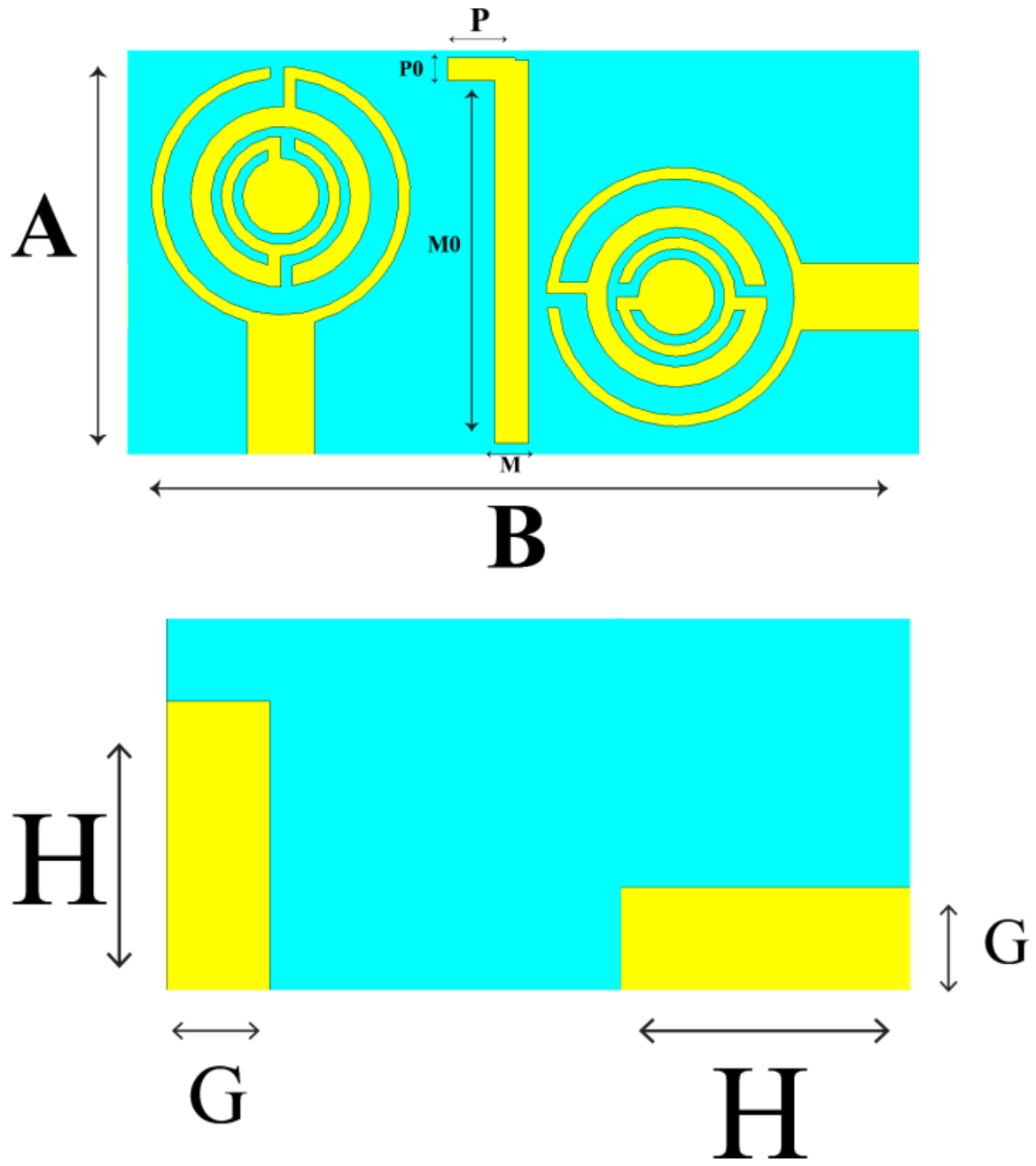
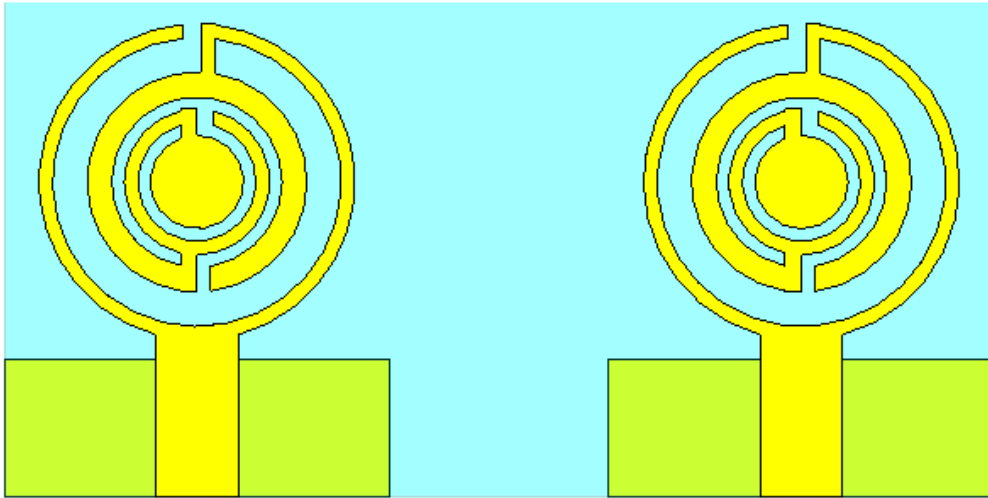


Figure 3.1: Geometry of the proposed antenna (A) front view(B) back view.

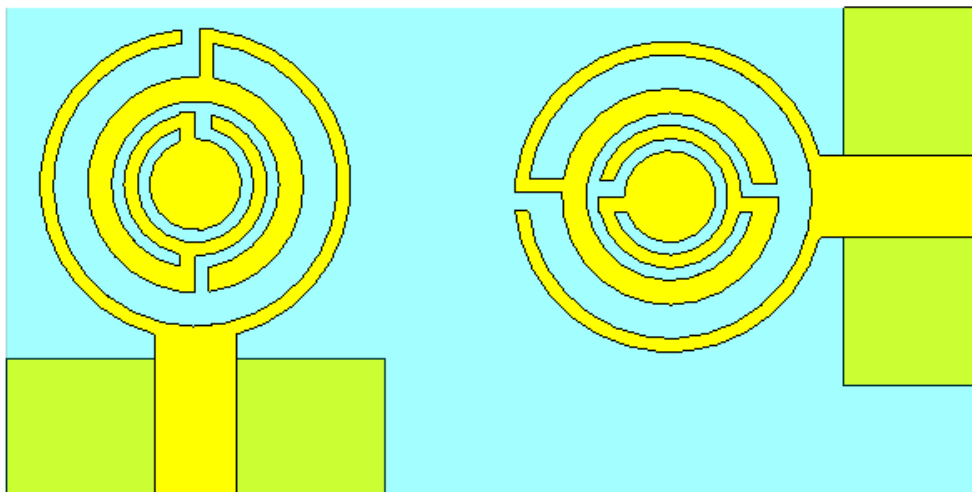
Parameter	A	B	G	M	M0	P	P0
Value(mm)	14	18	14	1.5	17	3	1

Table 3.1: Geometric dimensions of the proposed antenna

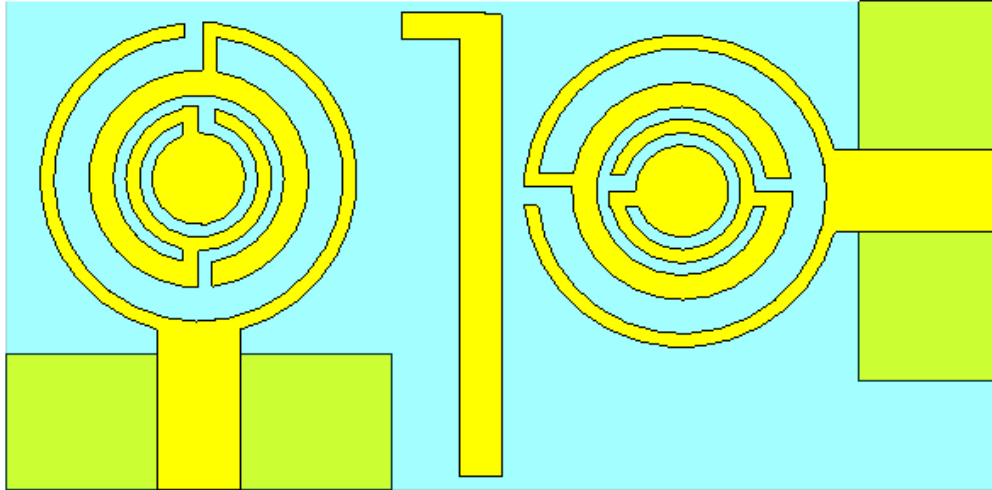
Usually, the design of a MIMO antenna needs to consider the issue of isolation. Several methods have been used to improve the isolation, such as increasing the distance between the antenna units, adding a decoupling structure or a metal isolation bar. However, the orthogonal placement is used in this work to improve the isolation of the designed antenna. Compared with other methods, this method can achieve a more compact structure without enlarging antenna size, reducing antenna performance, and affecting the impedance matching of the antenna.



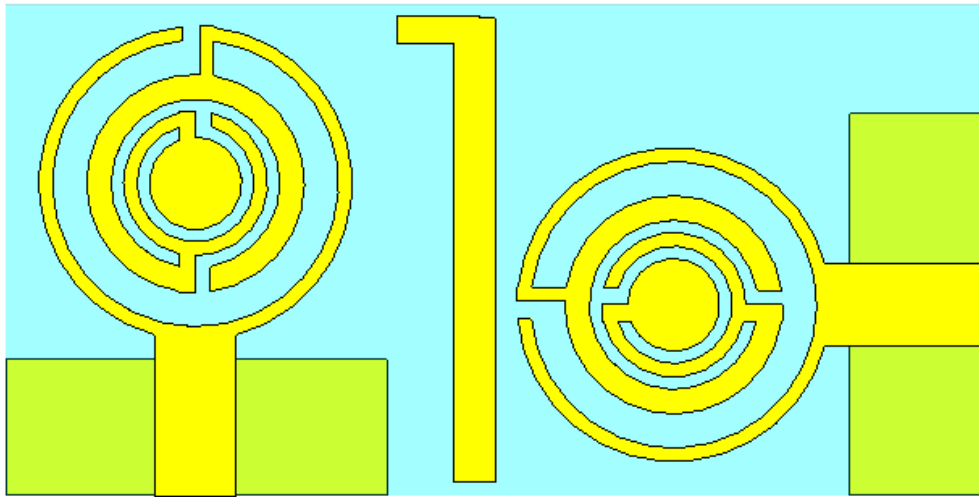
Step-1



Step-2



Step-3



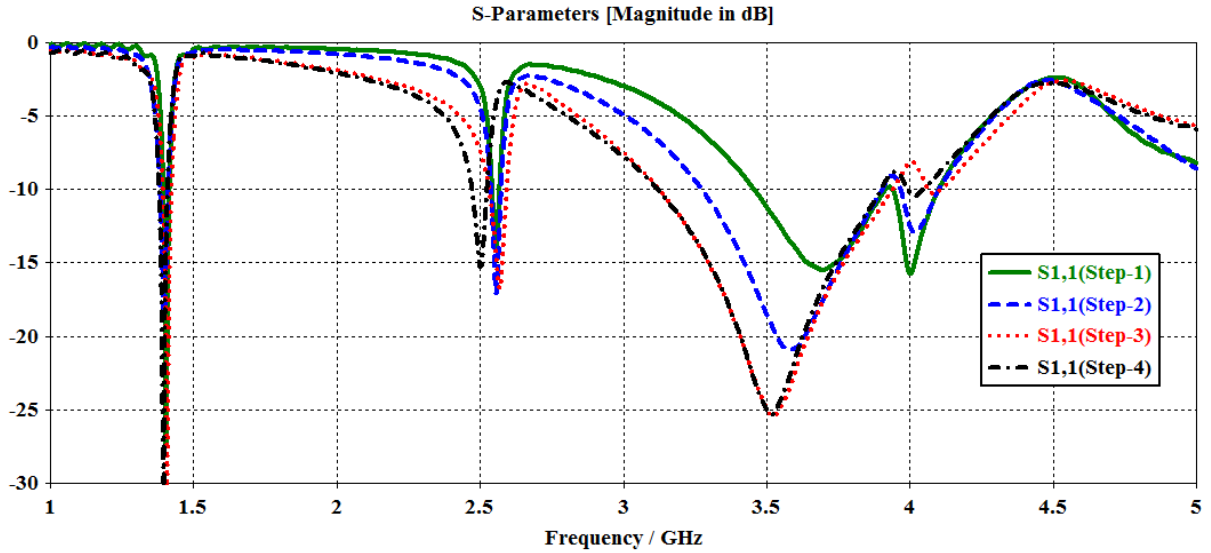
Step- 4

Figure 3.2: Evolution structures of the proposed Quad band-MIMO antenna

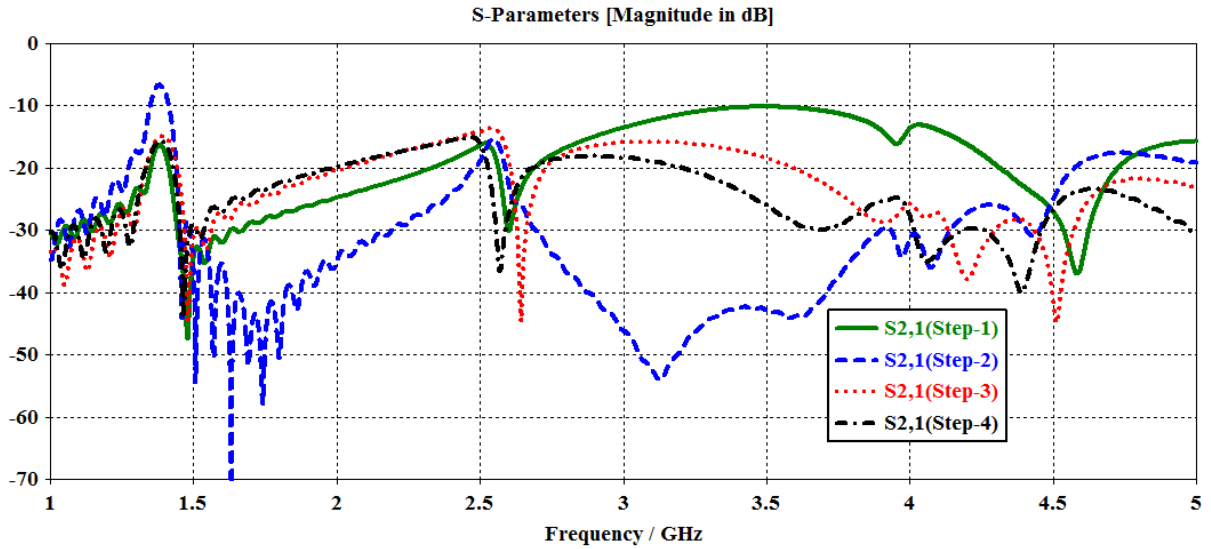
The evolution process of the design quad band MIMO antenna is shown in Figure 3.2. Initially, two identical quad band spiral monopole antenna elements are placed parallel to each other as illustrated in step 1 in Figure 3.2. Then, a second antenna is placed orthogonally (90° with respect to the first antenna) as illustrated in Figure 3.2(Step-2). Next, an inverted L shaped bar is placed between two antennas (Step-3) as depicted in Figure 3.2. Finally, in the last stage the horizontal antenna is shifted to lower side as presented in (Step-4) Figure 3.2

Figure 3.3 shows the respective S_{11} and S_{21} responses (versus frequency) for the different stages of the proposed MIMO antenna. From the plot; in step 1 the design exhibits the four

bands at 1.39, 2.55, 3.70 and 4.01 GHz. a very poor isolation through the operating bands especially the third and the fourth. In the next step, the antenna exhibits four bands, also the mutual coupling ($|S_{12}|$) decreased noticeably to less than -14 dB except the lower frequencies. The third step the antenna provides a four bands for WiMAX and C band and mutual coupling reduction is obtained (< -20 dB) except in the second band. Finally, step 4 the antenna has four bands with good matching and the isolation is less than -15 dB four all bands.



(A)



(B)

Figure 3.3: Simulated (a) S11 (dB) (b) S21 (dB) response for different stages of the proposed MIMO antenna.

3.3 Results and discussions

3.3.1 The input reflection coefficient

The input reflection coefficient of the optimum final structure is presented in Figure 3.4(a). The structure behaves as a quad band at 1.39GHz, 2.5GHz, 3.52GHz and 4.02GHz for WiMAX and C band applications.

The simulated transmission coefficient is depicted in Figure 3.4(b). It is clearly seen from the figure that the isolation between the two antennas is high approximately (≤ -15 dB) and covers the quad bands.

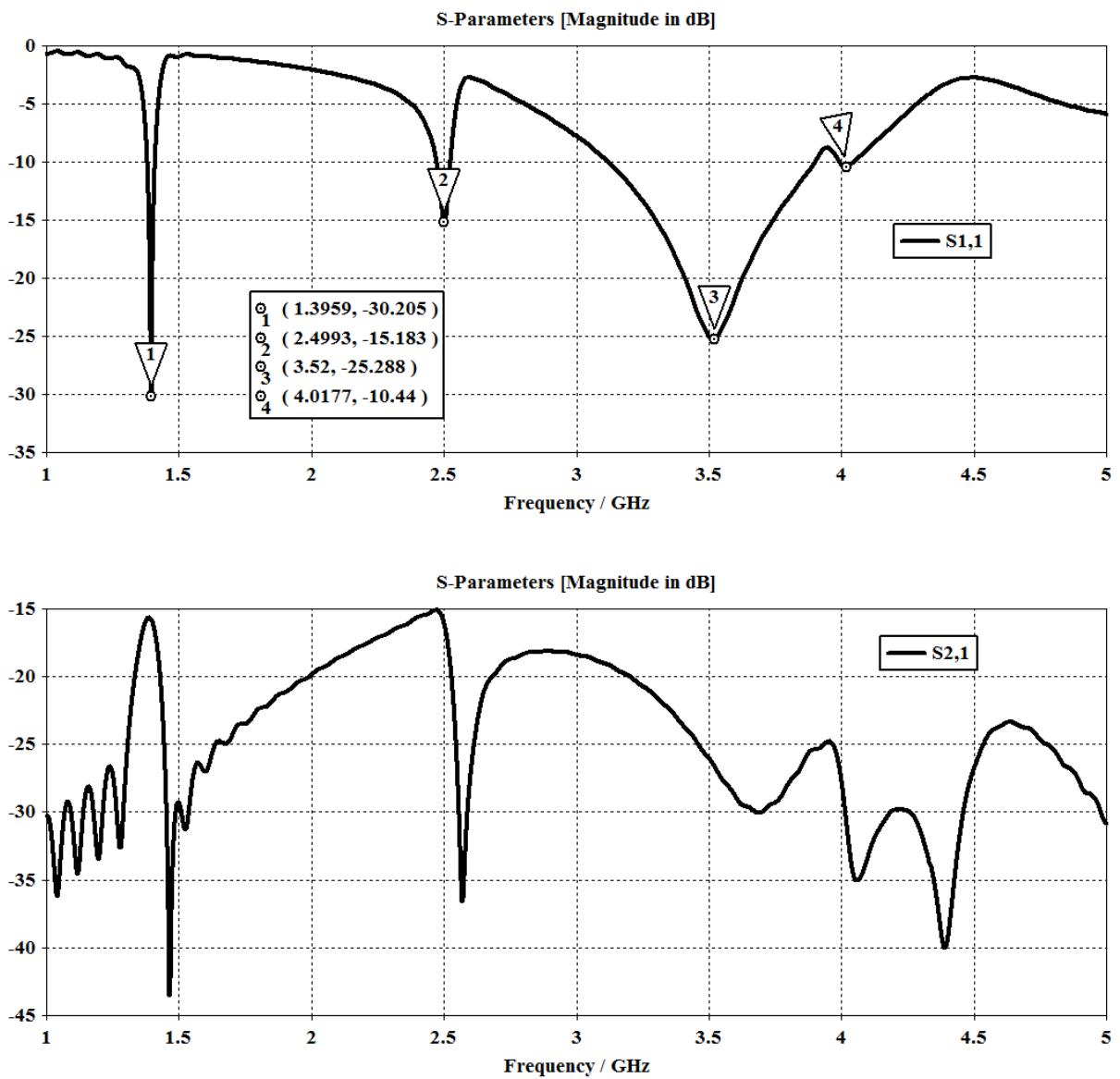


Figure 3.4: Simulated $S_{1,1}$ & $S_{2,1}$ of the final structure.

3.3.2 Parametric study

To further investigate the Quad band MIMO antenna performance (inverted L-shaped in isolation), a parametric study is carried out.

- **Effect of M_0 :**

Figure 3.5 shows the results obtained through simulation of the S-parameters (S_{11}/S_{21}) characteristics according to the changes in the M_0 inverted L-shaped branch length while the others parameters are kept constant. From the graph, as M_0 increases the third resonant frequency decreases whereas the other frequencies are not changed. The transmission coefficient shows that as M_0 increases the isolation is <-15 dB except at the first band.

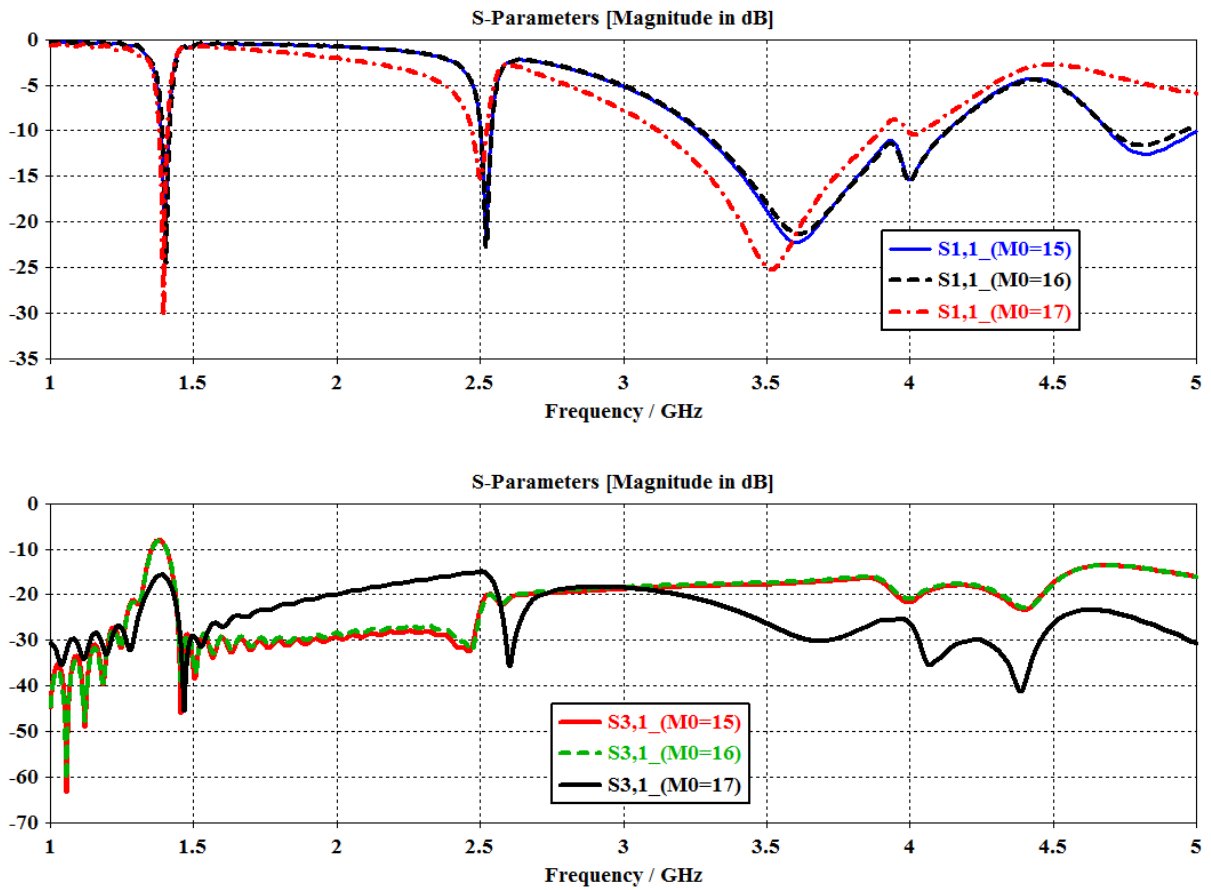


Figure 3.5: Simulated S_{11}/S_{21} for different values of M_0

- **Effect of M**

Figure 3.6 shows the antenna return loss for different values of the thickness M of an inverted L-shaped stub. It is seen that by increasing M , the four resonant frequencies are kept unchanged for input reflection coefficient. In the transmission coefficient as M increases the isolation in the second band >-15 dB. For M equal 1.5 mm, the isolation is less -15 dB for all bands.

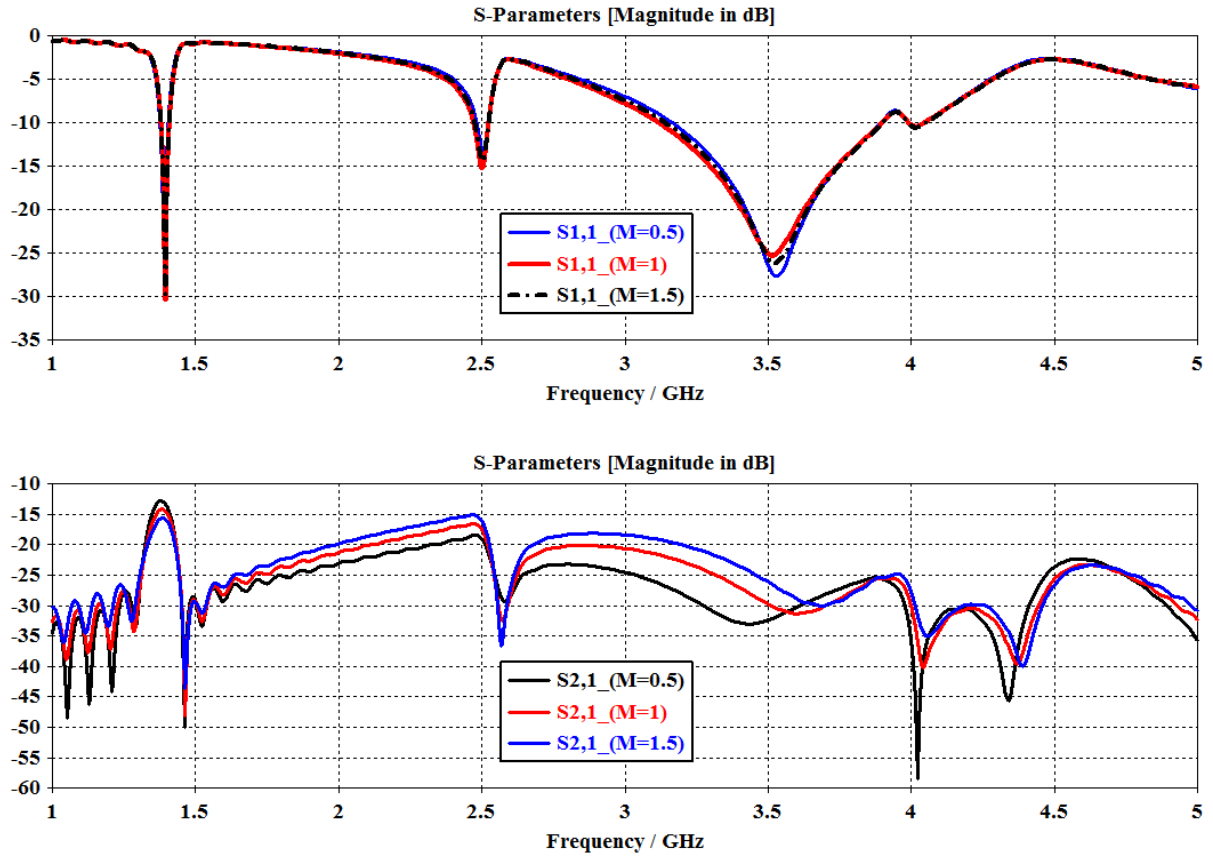
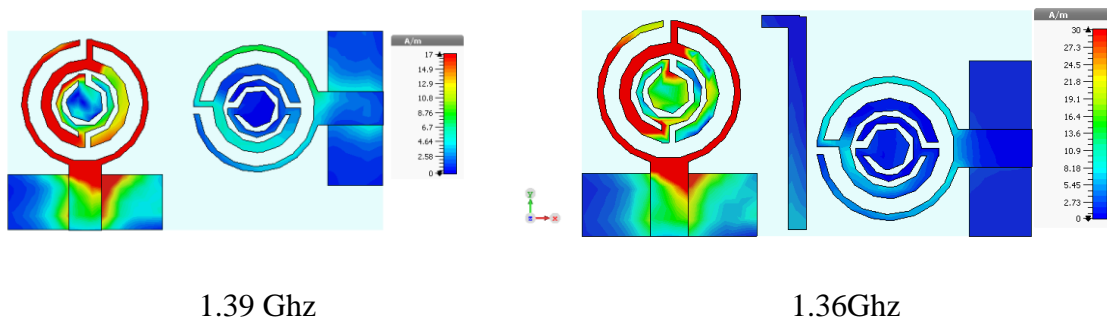


Figure 3.6: Simulated S_{11}/S_{21} for various M

3.3.3 The current distribution

To further understand the decoupling effect between antenna elements, the surface current distributions at the four bands are depicted in Figure 3.7. When port 1 is excited and port 2 is matched by $50\ \Omega$ load (vice-versa when port 2 is excited).



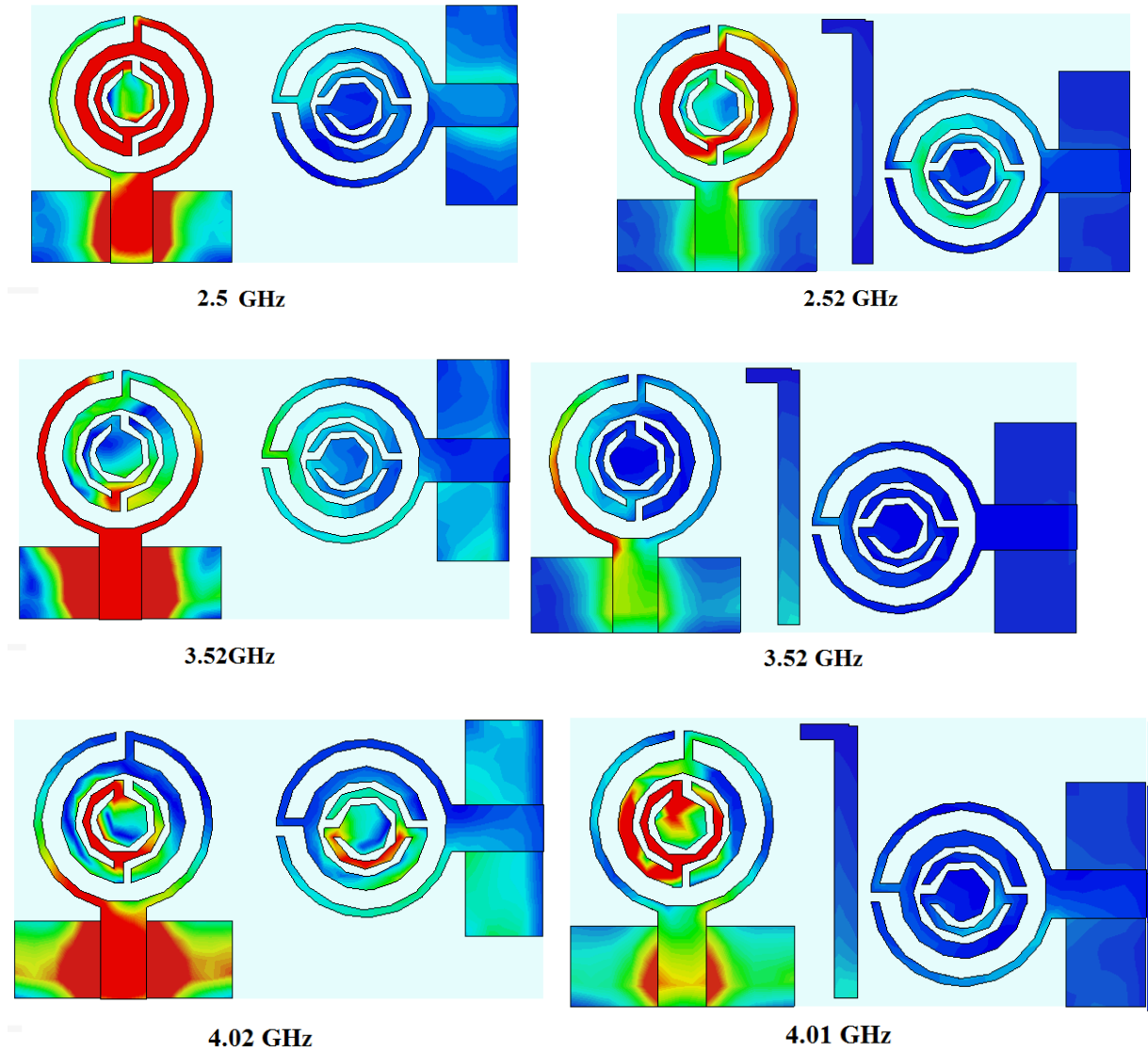


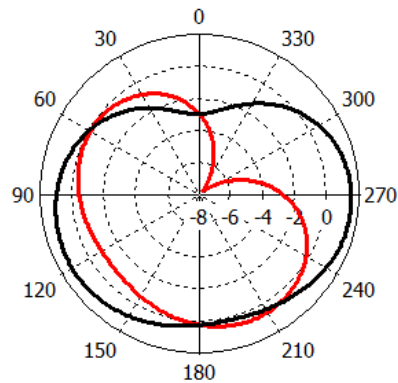
Figure 3.7: The surface current density of the proposed quad band MIMO antenna.

When the MIMO antenna is excited at port 1 without isolation (inverted L shaped stubs), the surface current of port 1 has a high tendency to couple with port 2 through the mutual coupling (vice-versa when port 2 is excited). It is also observed that with isolation stub, the surface current is strongly excited in inverted L-shaped stubs, which results in better inter-port isolation and there by significantly improves the diversity performance of the quad band MIMO antenna

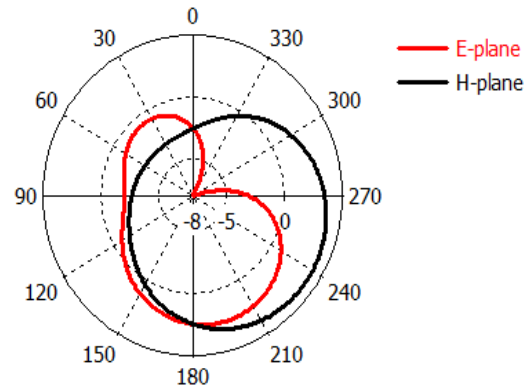
3.3.4 The radiation pattern

Figure 3.8 shows the simulated radiation patterns containing E-plane and H-plane (x-z plane) and E-plane y-z plane) at the 1.39, 2.5, 3.52 and 4.03 GHz. One of the two ports is excited and the other port terminated with 50- Ω matched load.

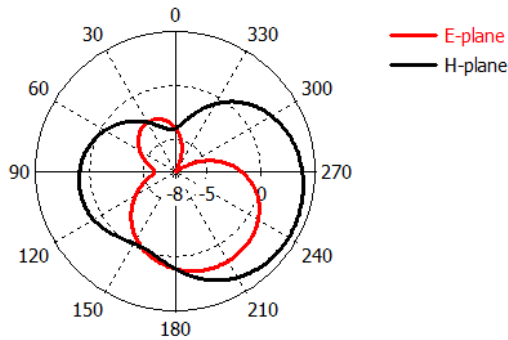
From the graph, it is observed that the radiation patterns are almost Omni-directional at the four frequencies and bidirectional in E-plane was observed at all frequency bands. The simulated realized gain is shown in figure 3.9. And maximum gain is 1.2dB



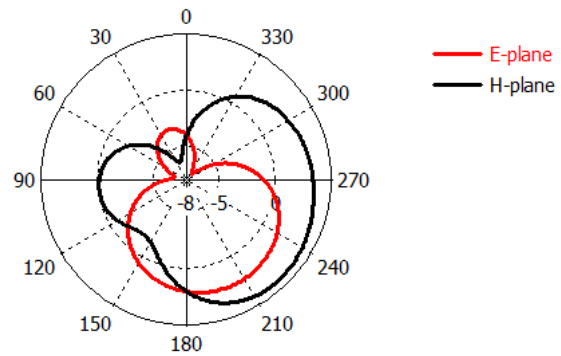
1.39 GHz



2.5 GHz



3.5 GHz



4.02 GHz

Figure 3.8: Simulated radiation patterns of the proposed MIMO antenna at 1.39, 2.5, 3.5 and 4.02 GHz for port-1.

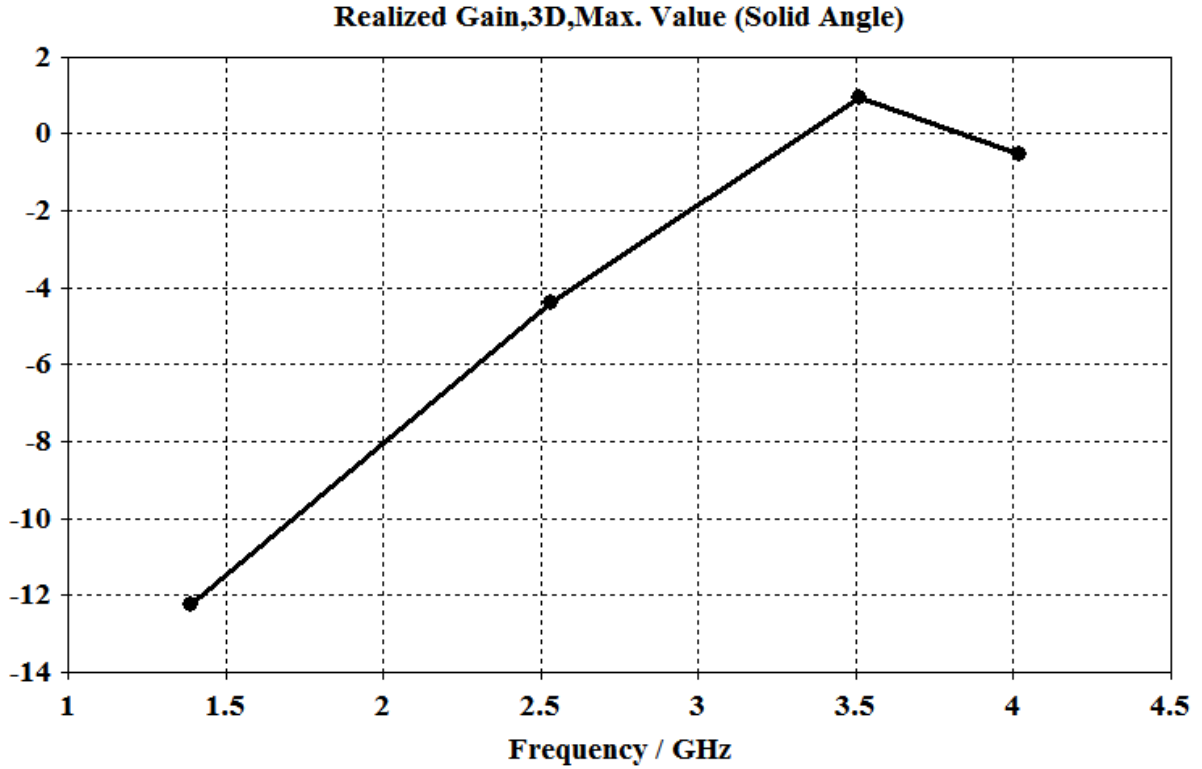


Figure 3.9: Realized gain characteristics of the proposed MIMO antenna.

Envelope Correlation Coefficient is an important parameter which indicates the diversity performance and pattern independence of the elements of the antenna. For the two port MIMO antenna, ECC can be obtained from the following equation using S-parameters [1].

$$ECC = \frac{|S_{11}^* S_{12} + S_{21}^* S_{22}|^2}{\left(1 - (|S_{11}|^2 + |S_{21}|^2)\right) \left(1 - (|S_{22}|^2 + |S_{12}|^2)\right)}$$

The value of ECC should ideally be zero for an uncorrelated MIMO antenna. However, for practical circumstances, the preferred limit is $ECC < 0.5$. Figure 3.10 presents the graph of ECC versus frequency of the proposed quad band MIMO antenna. From the figure it is observed that the $ECC < 0.2$ over the four operating bands of the proposed MIMO antenna, which is so far below the accepted value 0.5.

Diversity gain is also an important parameter to evaluate the diversity performance of the antenna. The relation to calculate DG of the MIMO antenna is as given below[2]:

$$DG = 10\sqrt{1 - (ECC)^2}$$

The diversity gain is also simulated and it is varying around 10 dB over the four operating bands of the MIMO as observed in Figure 2.11.

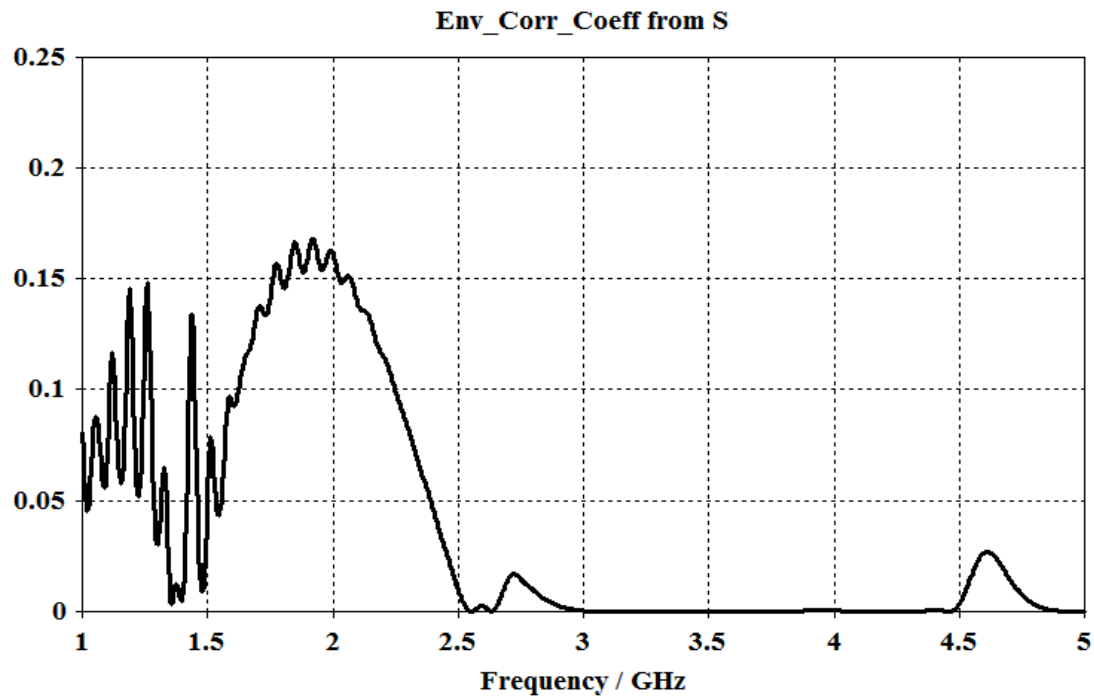


Figure 3.10: Simulated ECC for the proposed MIMO antenna

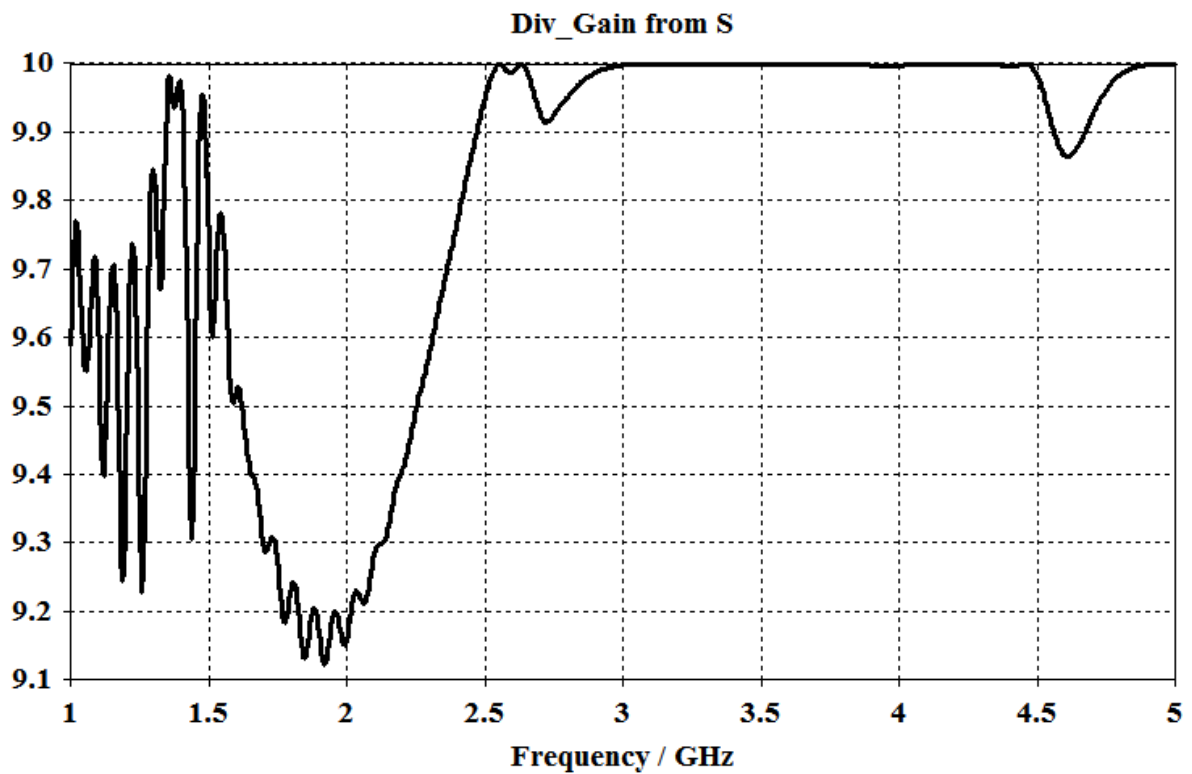


Figure 3.11. Diversity gain of the proposed MIMO antenna.

Finally, Table 3.2 shows the comparison of the proposed quad band MIMO antenna with other MIMO antennas reported in literature in terms of frequency band, overall size, and isolation achieved. From the table, it can be observed that the overall area of the proposed MIMO antenna is less than many of the reported antennas. Moreover, the proposed antenna exhibits multiband characteristics with good isolation between the individual antenna elements.

Table 3.2: Comparison of different antennas with the designed antenna

Ref.	Size in mm ²	Operating frequency in GHz	Isolation (dB)	ECC	applications
[3]	52 × 77.5	2.4	15	<0.05	WLAN
[4]	70 × 70	1.8/3.6/5.4/7.2	15	<0.3	GSM II,WLAN,WiMAX
[5]	50 × 100	1.75/3/4.5/6	14	<0.3	C band
[6, 7]	80 × 35	UWB	15	≤0.005	-
This work	36×18	1.39/2.5/3.52/4.03	≤15	≤0.3	WiMAX,Cband

References

- [1] H. S. Singh, G. K. Pandey, P. K. Bharti, and M. K. Meshram, "Design and performance investigation of a low profile MIMO/Diversity antenna for WLAN/WiMAX/HIPERLAN applications with high isolation," *International Journal of RF and Microwave Computer-Aided Engineering*, vol. 25, pp. 510-521, 2015.
- [2] M. S. Sharawi, *Printed MIMO antenna engineering*: Artech House, 2014.
- [3] S. R. Pasumarthi, J. B. Kamili, and M. P. Avala, "Design of dual band MIMO antenna with improved isolation," *Microwave and Optical Technology Letters*, vol. 61, pp. 1579-1583, 2019.
- [4] C. Rajagopal, N. Noorullakhan, S. B. Suseela, and R. Sankararajan, "Compact modified circular patch quad-band MIMO antenna with high isolation and low correlation," *International Journal of Microwave and Wireless Technologies*, vol. 9, pp. 581-590, 2017.
- [5] Y. K. Choukiker, S. K. Sharma, and S. K. Behera, "Hybrid fractal shape planar monopole antenna covering multiband wireless communications with MIMO implementation for handheld mobile devices," *IEEE Transactions on Antennas and Propagation*, vol. 62, pp. 1483-1488, 2013.
- [6] F. Bahmanzadeh and F. Mohajeri, "Simulation and fabrication of a high-isolation very compact MIMO antenna for ultra-wide band applications with dual band-notched characteristics," *AEU-International Journal of Electronics and Communications*, vol. 128, p. 153505, 2021.
- [7] R. Gurjar, D. K. Upadyay, B. Kanaujia, and A. Kumar, "A compact U-shaped UWB-MIMO antenna with novel complementary modified Minkowski fractal for isolation enhancement," *Progress In Electromagnetics Research C*, vol. 107, pp. 81-96, 2021.

General Conclusion

This work focuses on study, design, fabrication and measurement of compact quad band MIMO monopole antenna for WiMAX and C band applications. The MIMO system contains two elements that are placed orthogonally.

In the first part, a compact quad band spiral shaped patch antenna have been proposed.

The proposed antenna exhibits a quad band by introducing a DMS defect on circular patch in the radiating element. The antenna resonates at 1.36GHz, 2.5GHz, 3.63GHz and 4.15GHz respectively, for WiMAX and C-band applications. The proposed antenna also provides a compact; a good radiation characteristic as well as stable gain compared with recent published works.

The work is extended to design and analysis of compact quad band MIMO antennas. The proposed design has a compact dimension of 18 mm \times 36 mm. Isolation between two ports is enhanced by the addition of an inverted L-shaped inserted on the top of substrate between antenna elements which are orthogonally placed. The obtained results show that the quad band MIMO antenna operates at 1.39GHz, 2.5GHz, 3.5GHz and 4.02GHz, respectively. The suggested quad band MIMO antenna shows a high isolation of 15.5dB. The antenna port envelope correlation coefficients are observed to be less than 0.2 in all frequencies of interest with diversity gain better than 10 dB. However, the maximum gain is 1.2 dB. The suggested future work on this subject is:

- Decrease the isolation of the proposed design less than 20dB.
- Design a compact 4 \times 4 quad band MIMO antenna with high isolation.